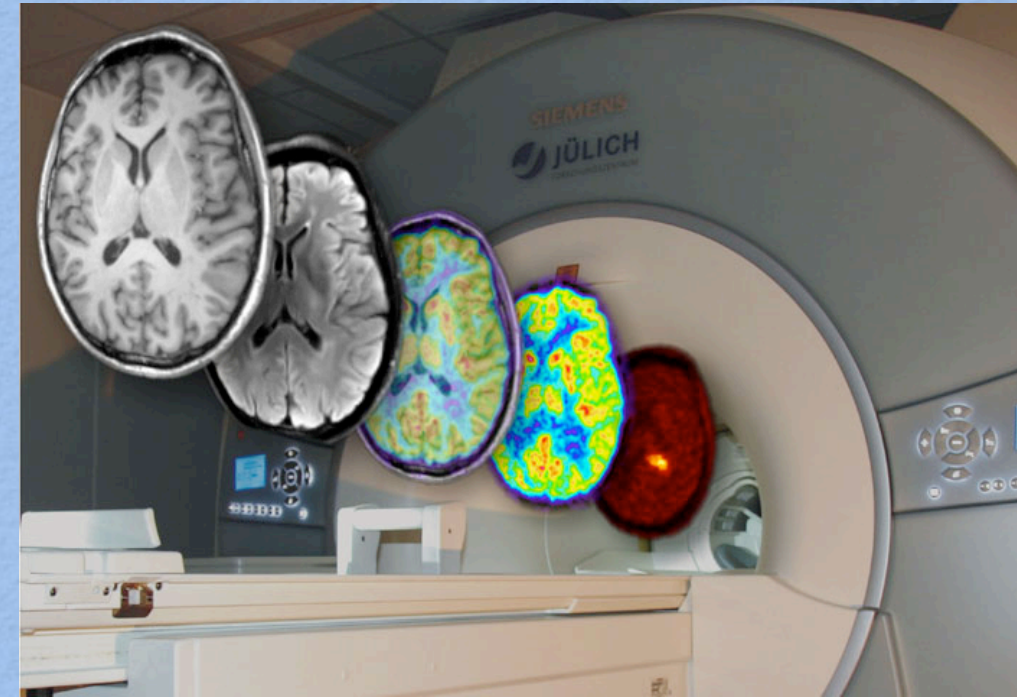


Spatial tomography of the proton from present data



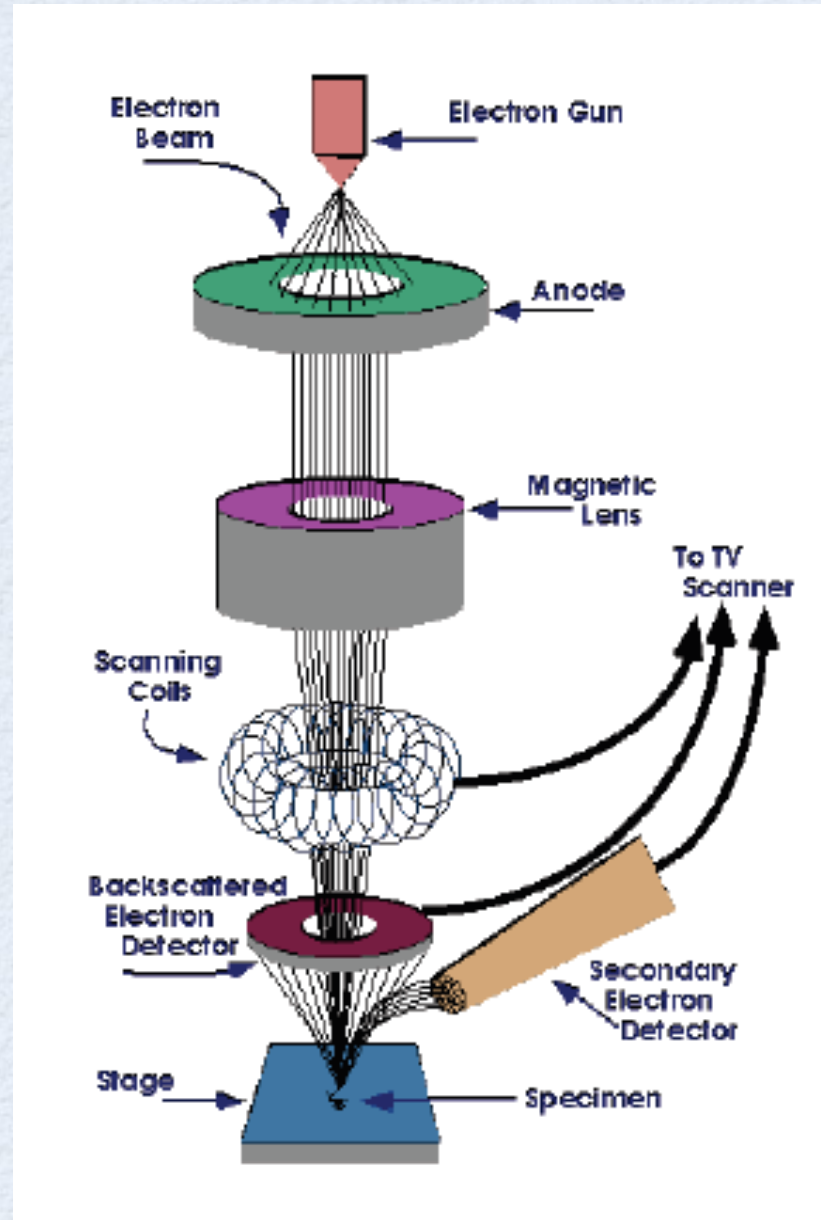
Marc Vanderhaeghen

INT Workshop “Spatial and Momentum Tomography of Hadrons and Nuclei”

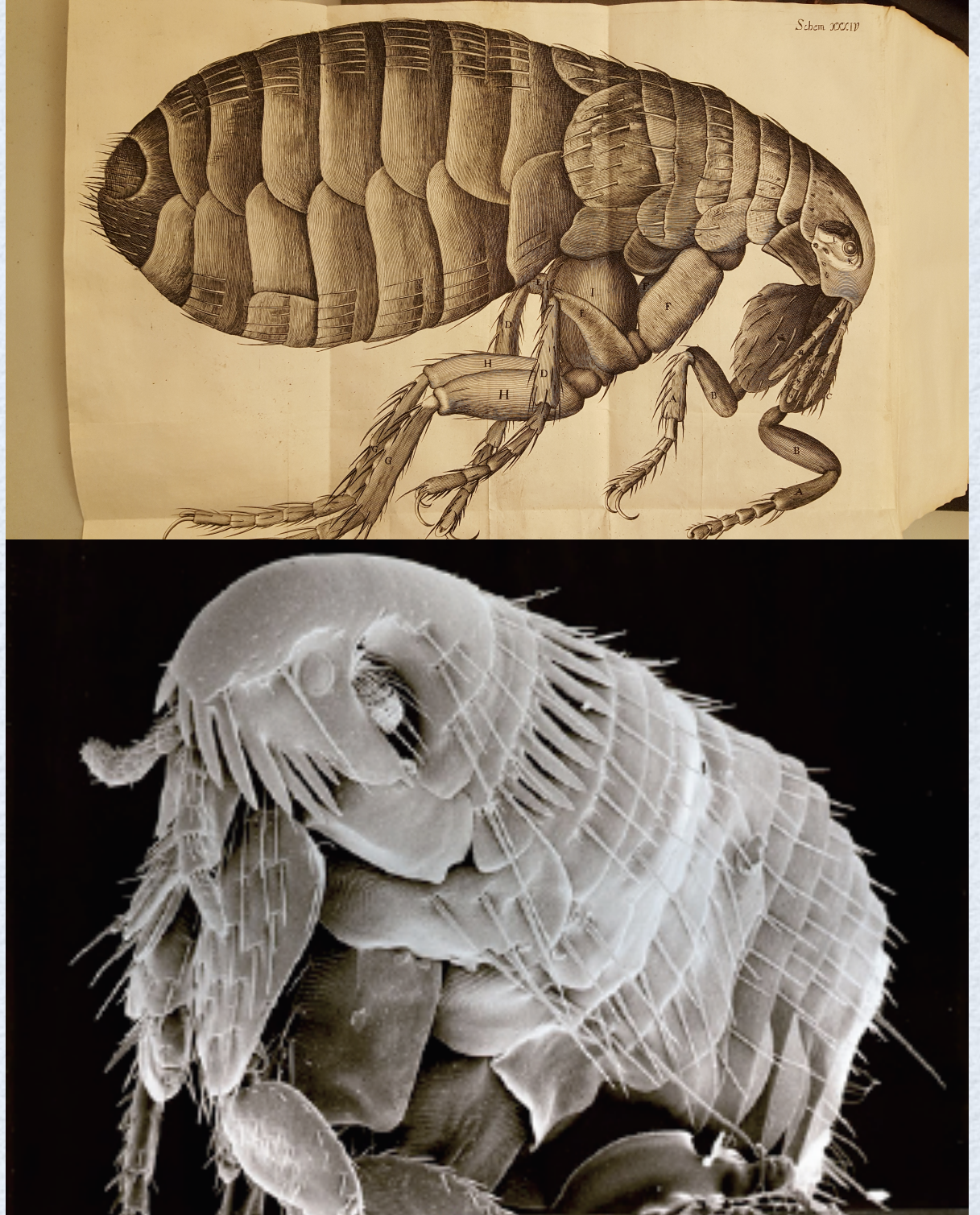
August 28 - September 29, 2017, Seattle, USA

how to image a system

R. Hooke (*Micrographia*, 1665)



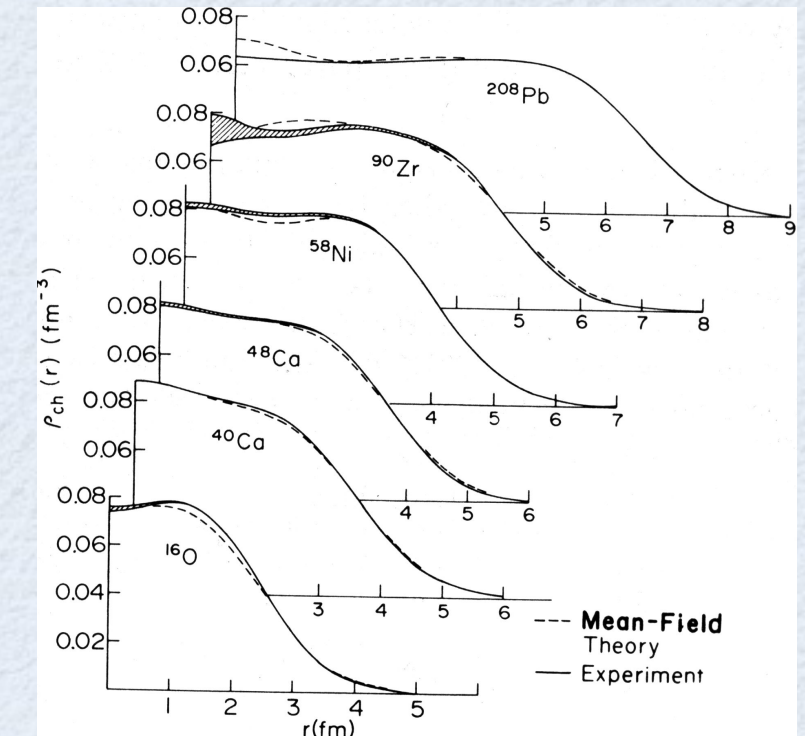
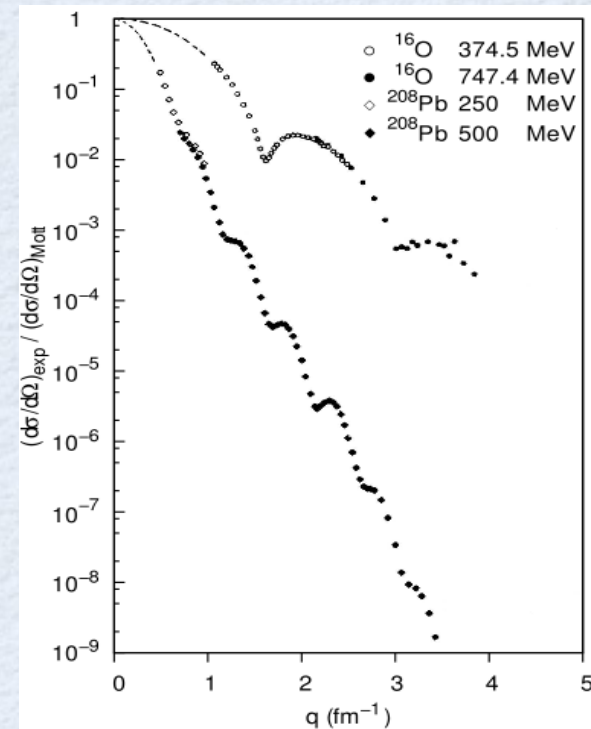
when target is static
($m_{\text{constituent}}, m_{\text{target}} \gg Q$)



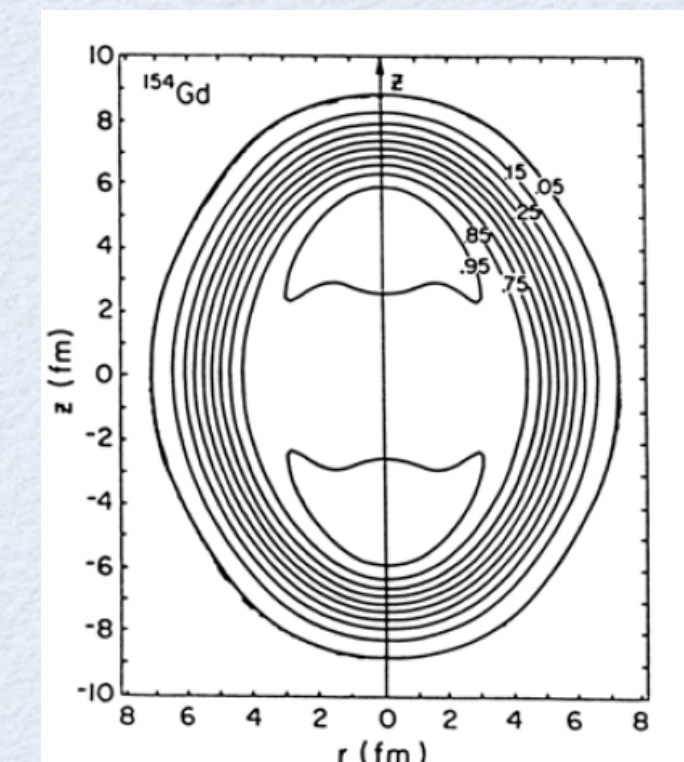
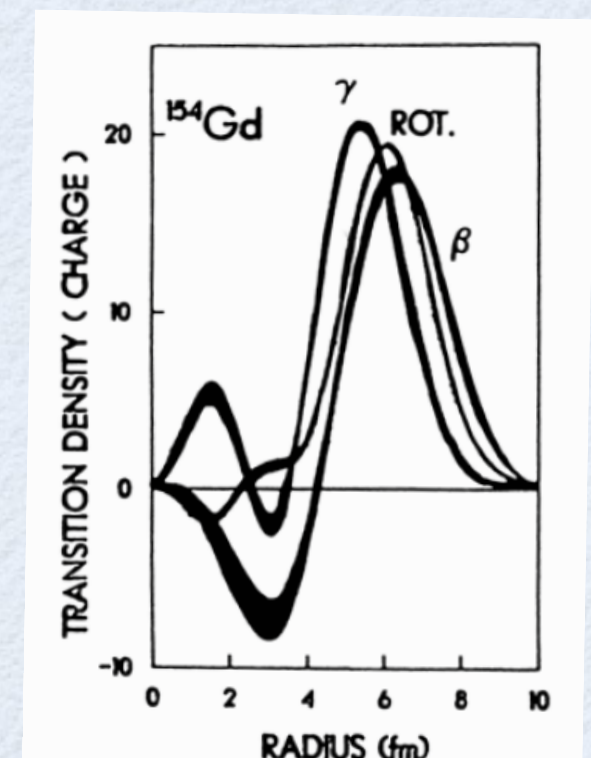
the 3D Fourier transform of form factors
gives the distribution of electric charge and magnetization

what do we know about spatial distributions of charges in nuclei?

sizes of nuclei:
as revealed through
elastic electron scattering

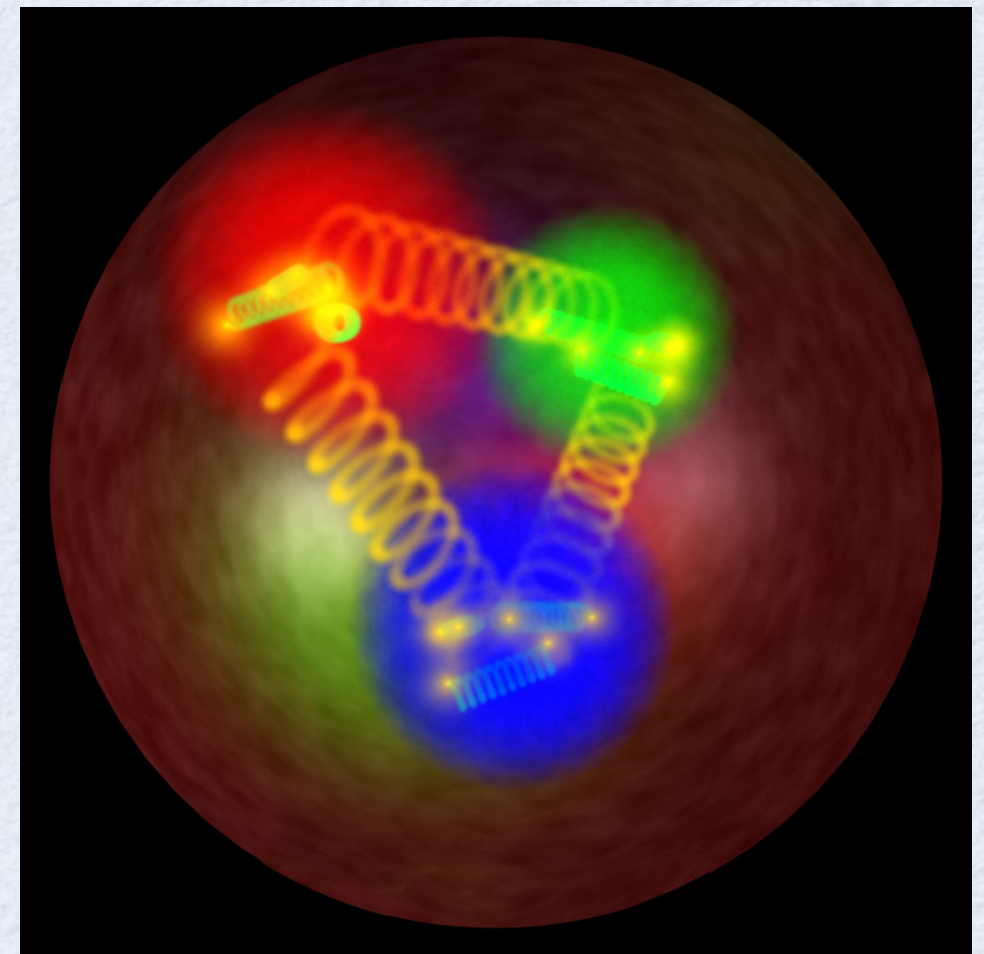


shapes of nuclei:
as revealed through
inelastic electron scattering

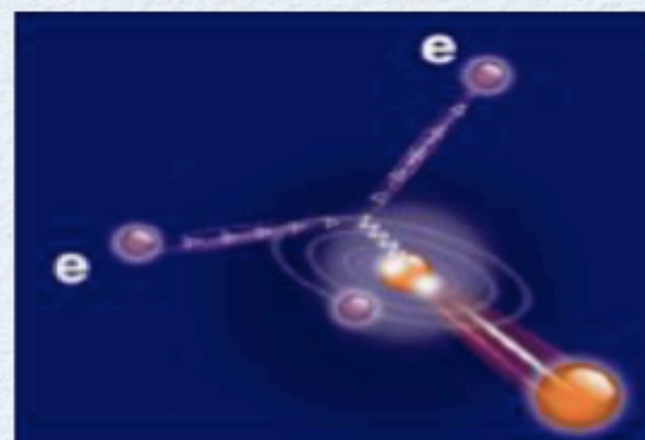
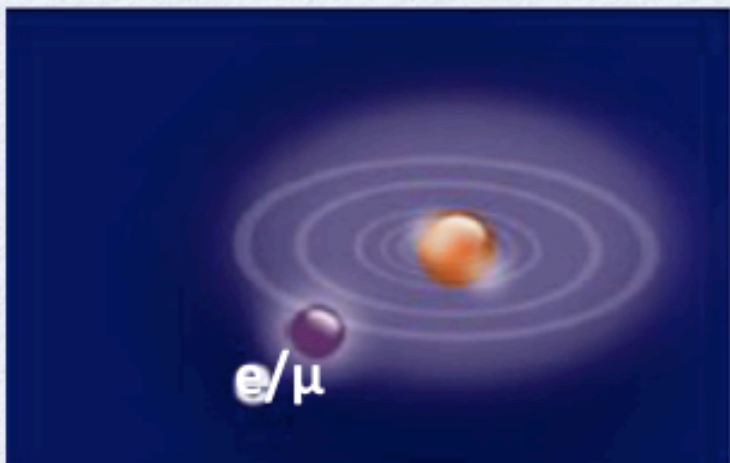


what do we know about the proton size and its charge distributions?

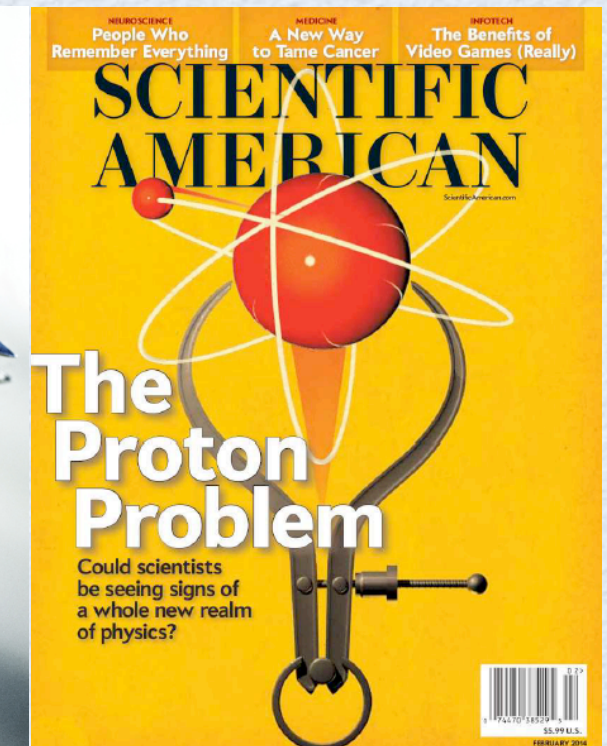
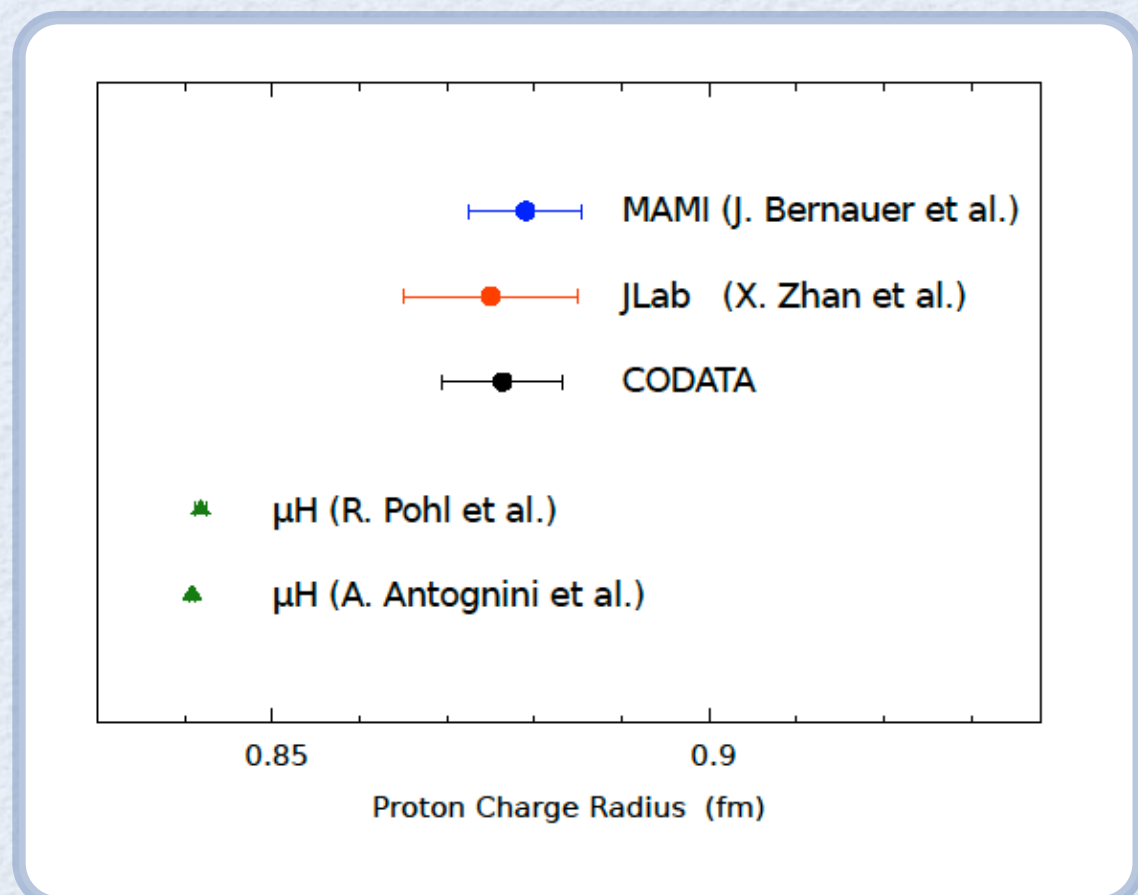
- proton **size**: charge radius R_E
very low Q^2 **elastic** electron scattering,
atomic spectroscopy (Lamb shift)
- proton **spatial (charge) distributions**
elastic electron scattering
e.m. FFs: $F_1(Q^2) \rightarrow \rho(b)$
- proton **3D transverse spatial/
longitudinal momentum distributions**
deeply virtual Compton scattering
GPDs $H(x, \xi, t) \rightarrow \rho(x, b)$ for $\xi=0$



proton size, proton radius puzzle



Proton radius puzzle



μH data:

Pohl et al. (2010)

Antognini et al. (2013)

$$R_E = 0.8409 \pm 0.0004 \text{ fm}$$



7 σ difference !?

ep data:

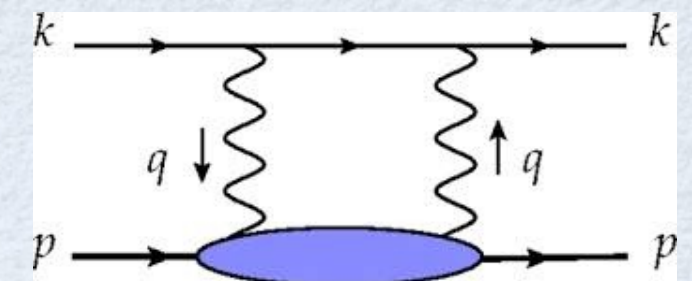
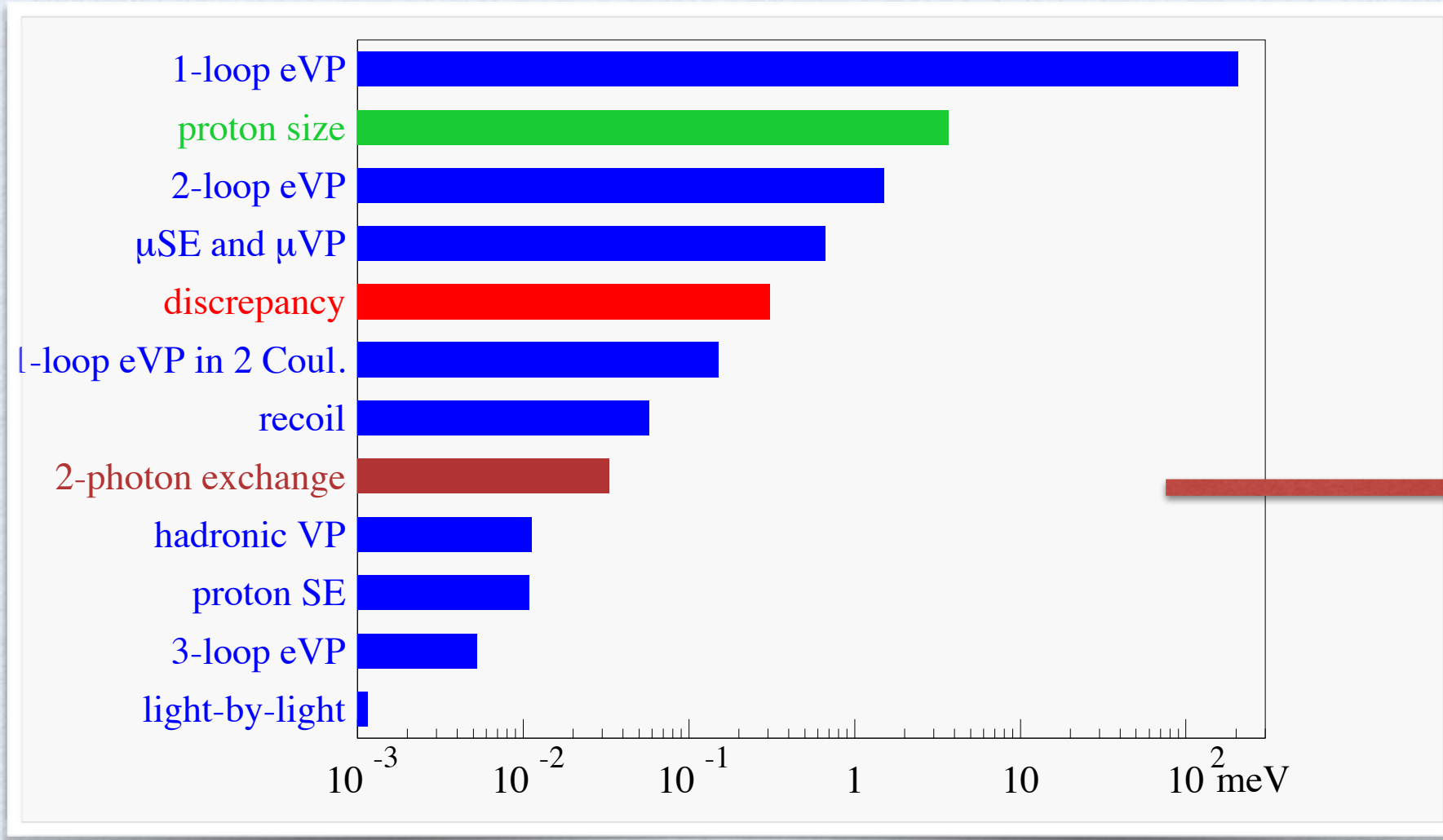
CODATA (2012)

$$R_E = 0.8775 \pm 0.0051 \text{ fm}$$



Lamb shift: status of known corrections

μH Lamb shift: summary of corrections



largest theoretical uncertainty

- elastic contribution on 2S level: $\Delta E_{2S} = -23 \mu\text{eV}$
- inelastic contribution: Carlson, vdh (2011) + Birse, McGovern (2012)

total hadronic correction on Lamb shift

$$\Delta E_{(2P - 2S)} = (33 \pm 2) \mu\text{eV}$$

...or about 10% of needed correction

Proton radius puzzle: what's next ?

→ μ atom Lamb shift: μD , $\mu^3\text{He}^+$, $\mu^4\text{He}^+$ have been performed

→ electronic H Lamb shift: higher accuracy measurements

→ electron scattering analysis:

- radius extraction fits (use fits with correct analytical behavior: 2π cut)
- radiative corrections, two-photon exchange corrections

new fit $R_E = 0.904(15) \text{ fm}$ (4σ from μH)

→ electron scattering experiments:

new G_{Ep} experiments down to $Q^2 \approx 2 \times 10^{-4} \text{ GeV}^2$

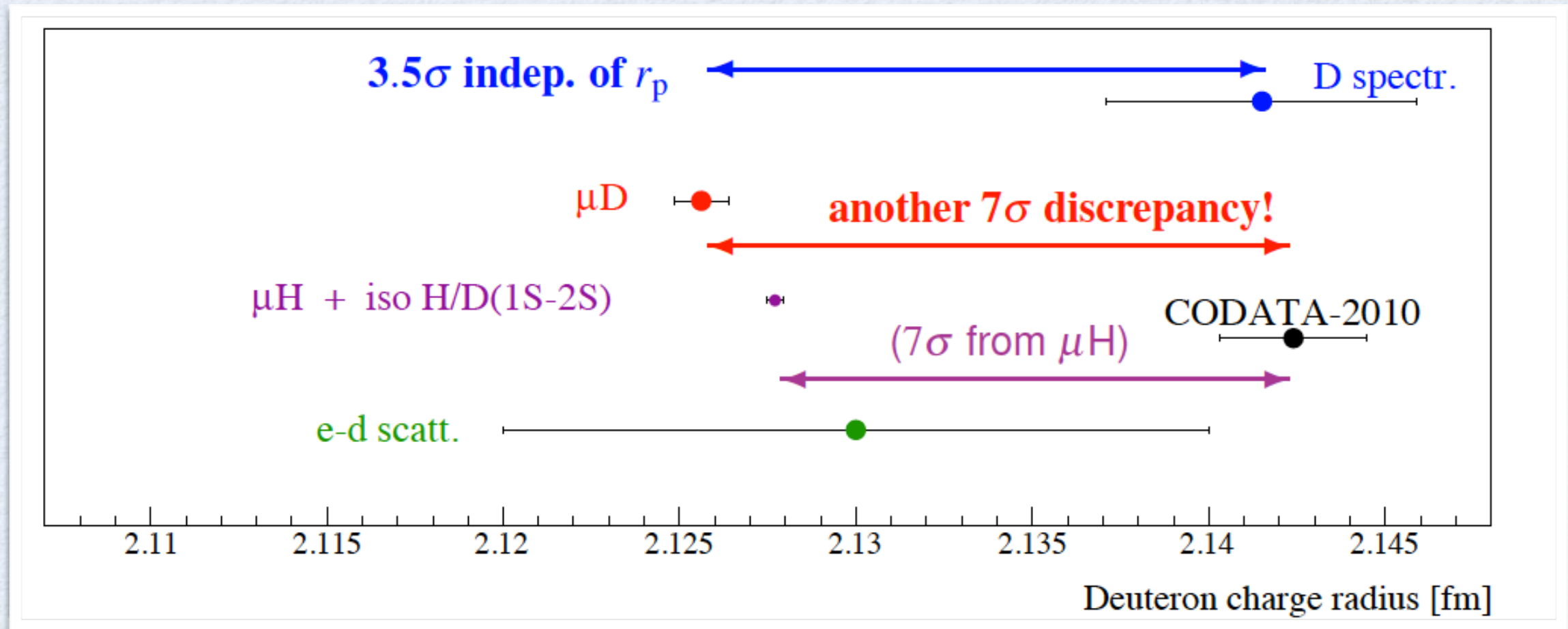
- **MAMI/A1**: Initial State Radiation (2013/4)
- **JLab/Hall B**: HyCal, magnetic spectrometer-free experiment, norm to Møller (2016/7)
- **MESA**: low-energy, high resolution spectrometers

→ muon scattering experiments: **MUSE@PSI** (2018/9)

→ e^-e^+ versus $\mu^-\mu^+$ photoproduction: lepton universality test

μ D Lamb shift experiment

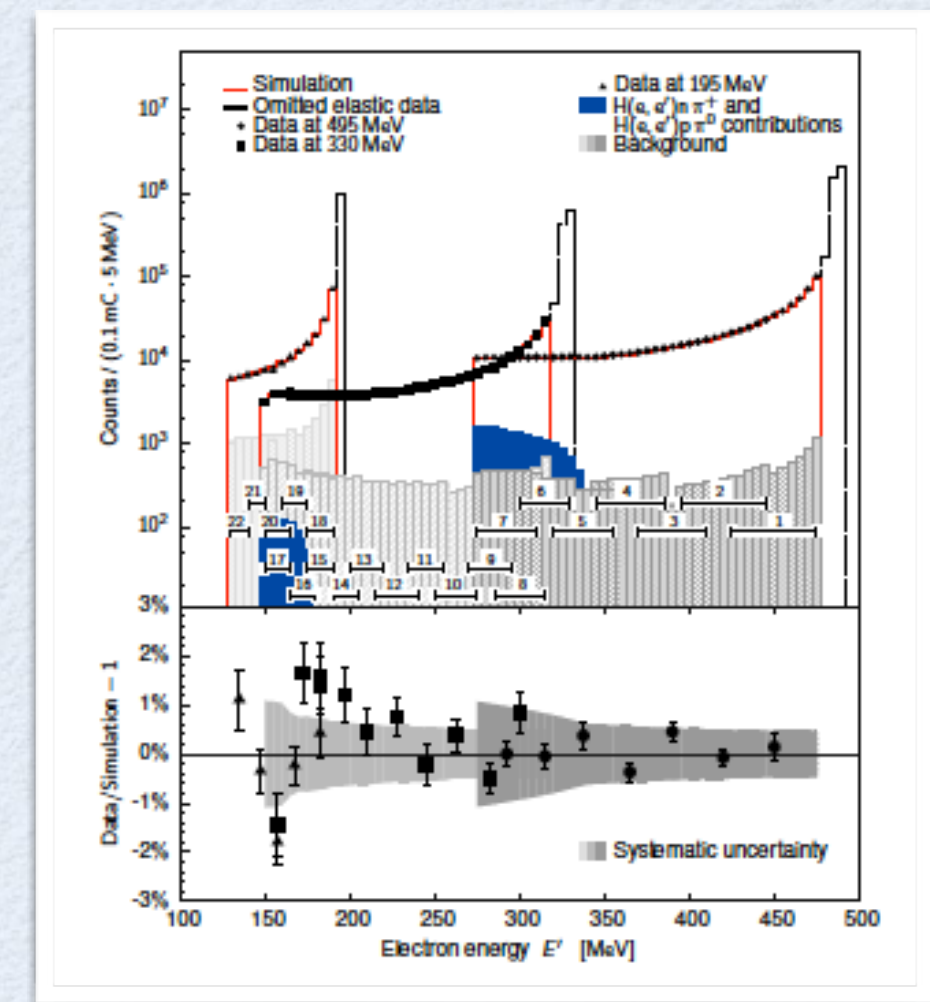
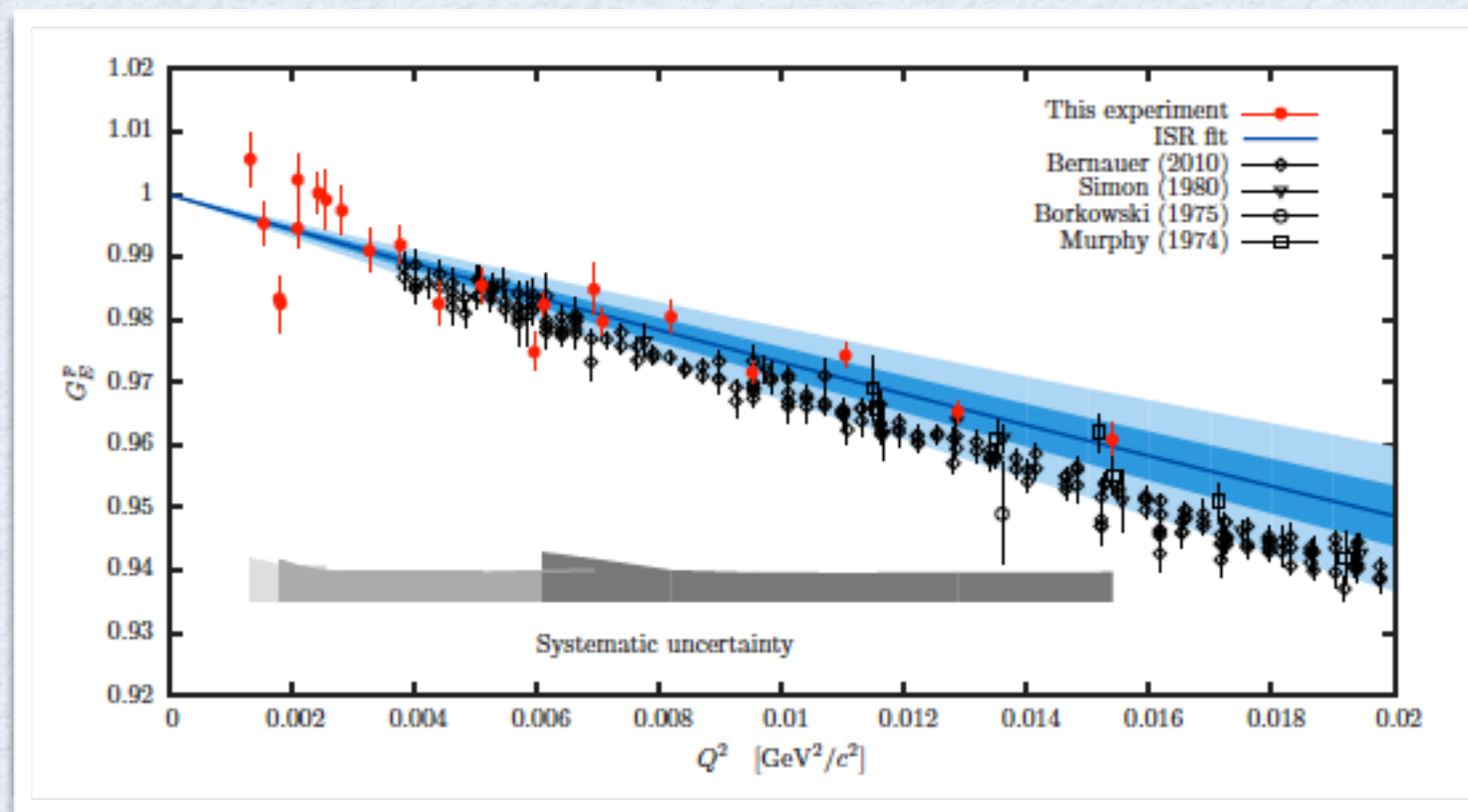
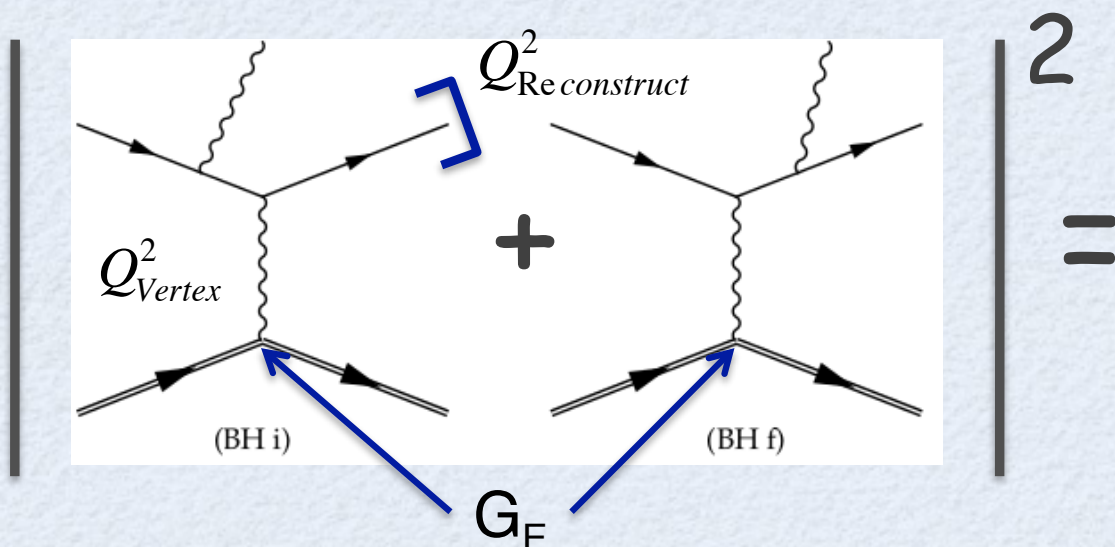
- H/D isotope shift (1S - 2S): $r_d^2 - r_p^2 = 3.82007 (65) \text{ fm}^2$ Parthey et al. (2010)
- CODATA 2010: $r_d = 2.14240 (210) \text{ fm}$
- r_p from μ H + isotope shift: $r_d = 2.12771 (22) \text{ fm}$
- new μ D Lamb shift @ PSI: $r_d = 2.12562 (13)_{\text{theo}} (77)_{\text{theo}} \text{ fm}$ Pohl et al., Science 353, 417 (2016)



- electronic D (r_p indep.): $r_d = 2.14150 (450) \text{ fm}$ ← 3.5 σ Pohl et al. (2016)
- improved radius measurement from e-d scattering was performed @ MAMI (2014)

ISR@MAMI experiment

- Extracting FFs from the radiative tail.
- Radiative tail dominated by coherent sum of two Bethe-Heitler diagrams.

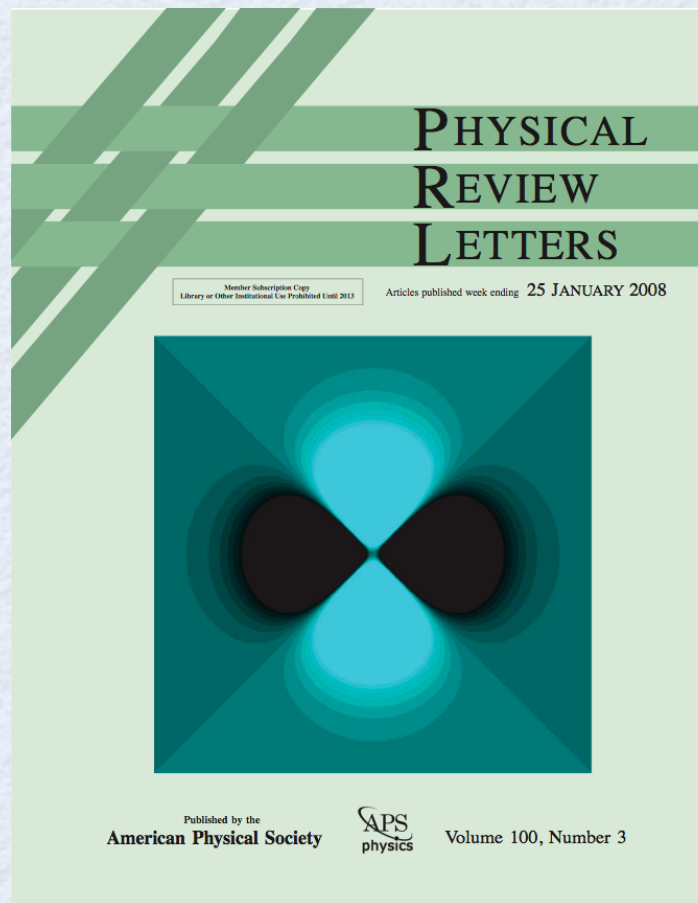


Mihovilovic et al. (2016)

good understanding of radiative tail ($\sim 1\%$)

follow up experiment:
down to $Q^2 \approx 2 \times 10^{-4} \text{ GeV}^2$

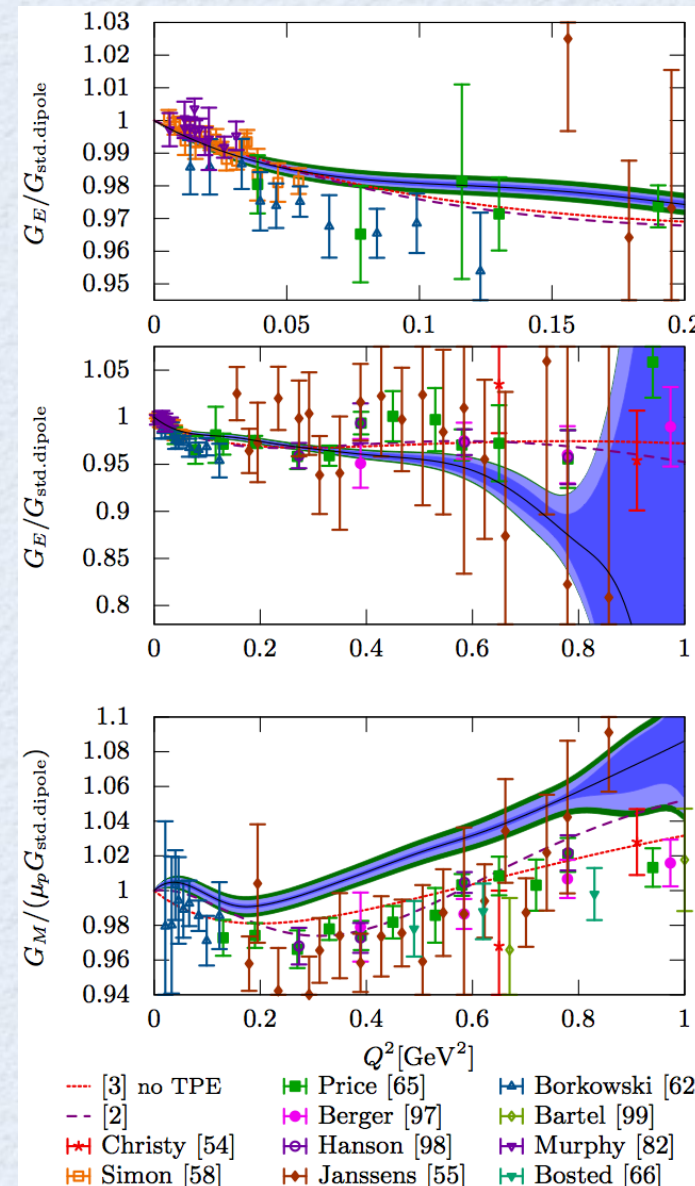
proton e.m. form factors, charge distributions



e^- scattering cross sections

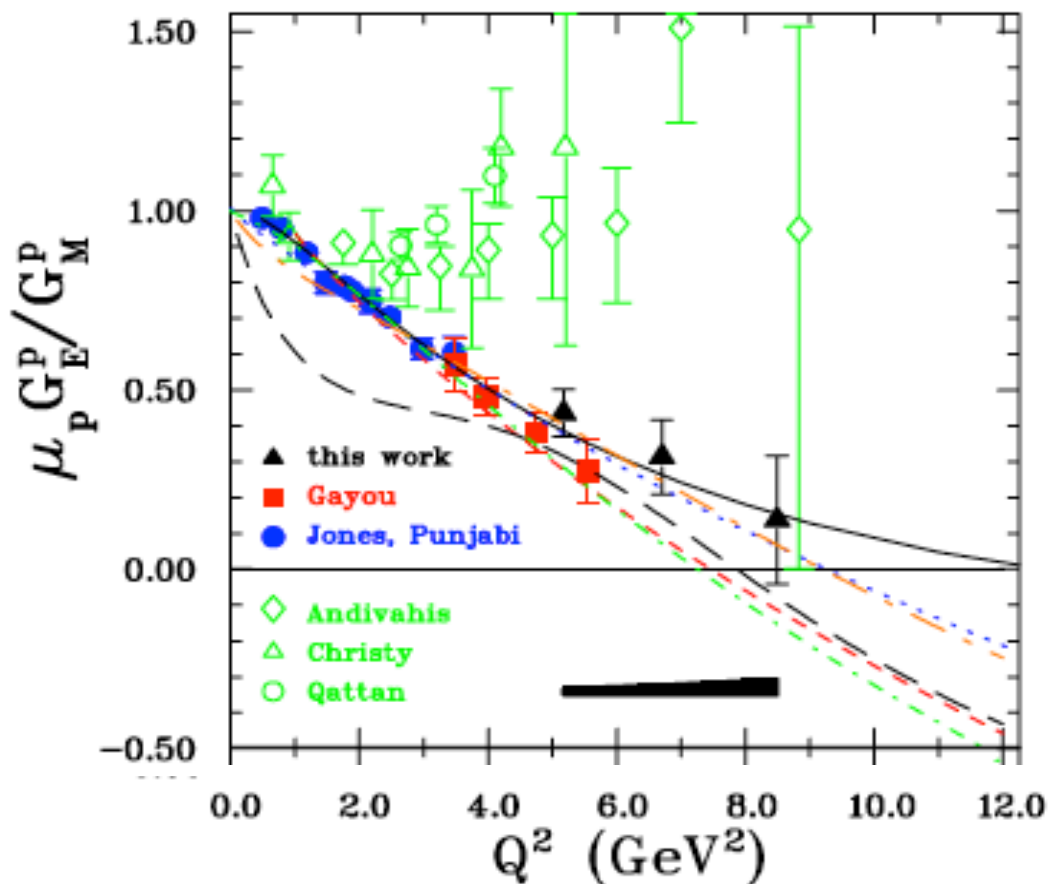
Electron scattering facilities JLab (12 GeV), MAMI (1.6 GeV):
uniquely positioned to deliver high precision data

MAMI/A1 achieved < 1% measurement
of proton charge radius R_E



Bernauer et al. (2010, 2013)

JLab polarization transfer measurements:
 G_{Ep} / G_{Mp} difference with Rosenbluth



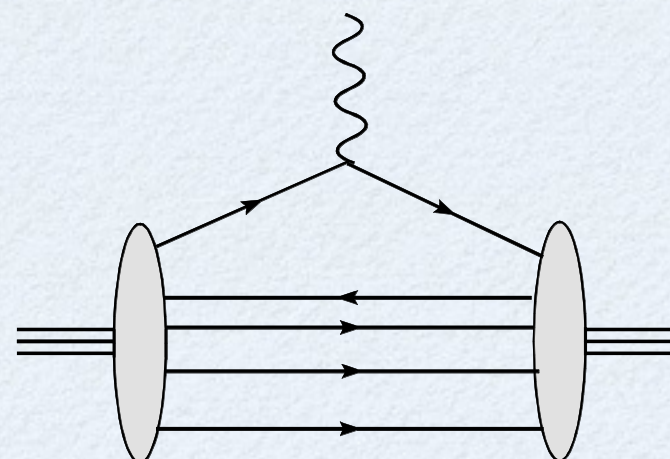
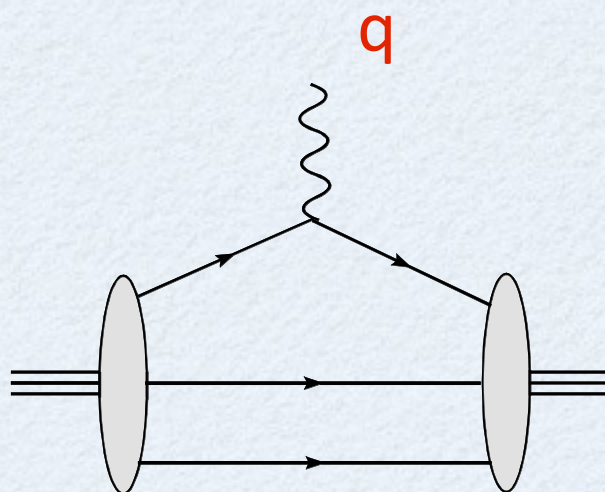
Jones et al. (2000)

Punjabi et al. (2005)

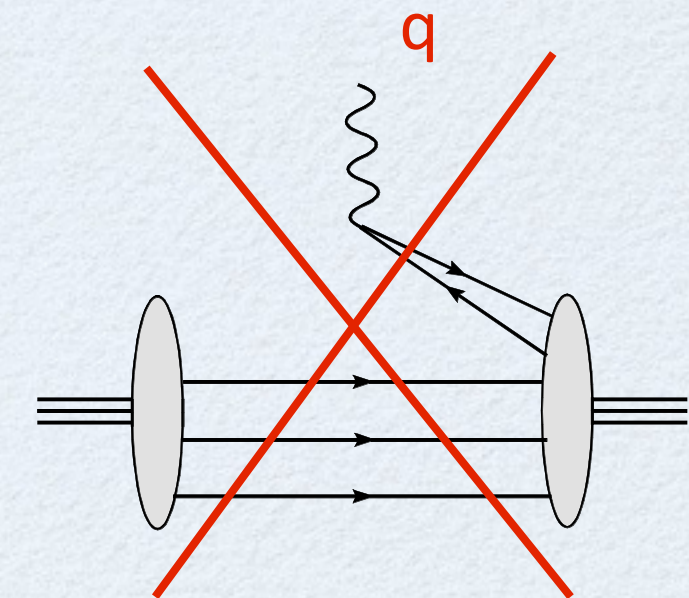
Gayou et al. (2002)

Puckett et al. (2010)

Interpretation of form factor as quark density



overlap of wave function
Fock components
with same number of quarks



overlap of wave function
Fock components
with different number of quarks
NO probability / charge density
interpretation

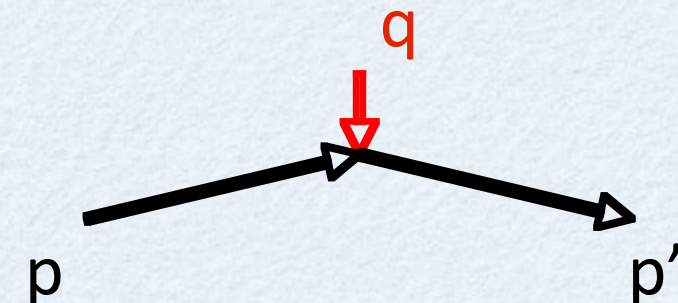
absent in a light-front frame!

$$q^+ = q^0 + q^3 = 0$$

quark transverse charge densities in nucleon (1)

→ light-front

$$q^+ = q^0 + q^3 = 0$$

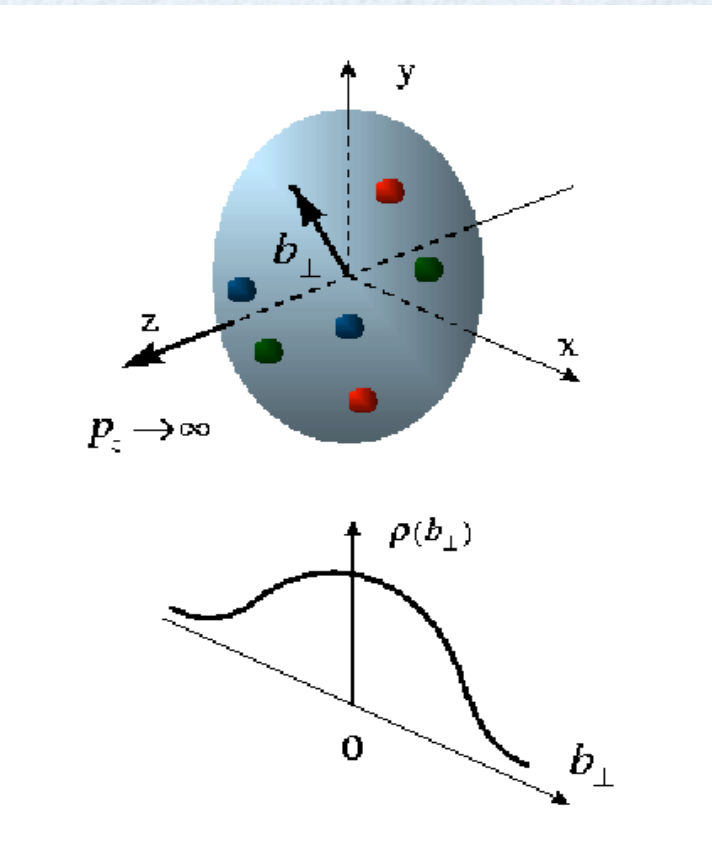


photon only couples to forward moving quarks

→ quark **charge density** operator

$$J^+ = J^0 + J^3 = \bar{q} \gamma^+ q = 2q_+^\dagger q_+$$

$$\text{with } q_+ \equiv \frac{1}{4} \gamma^- \gamma^+ q$$



→ longitudinally polarized nucleon

$$\begin{aligned} \rho_0^N(\vec{b}) &\equiv \int \frac{d^2 \vec{q}_\perp}{(2\pi)^2} e^{-i \vec{q}_\perp \cdot \vec{b}} \frac{1}{2P^+} \langle P^+, \frac{\vec{q}_\perp}{2}, \lambda | J^+(0) | P^+, -\frac{\vec{q}_\perp}{2}, \lambda \rangle \\ &= \int_0^\infty \frac{dQ}{2\pi} Q J_0(bQ) F_1(Q^2) \end{aligned}$$

Soper (1997)

Burkardt (2000)

Miller (2007)

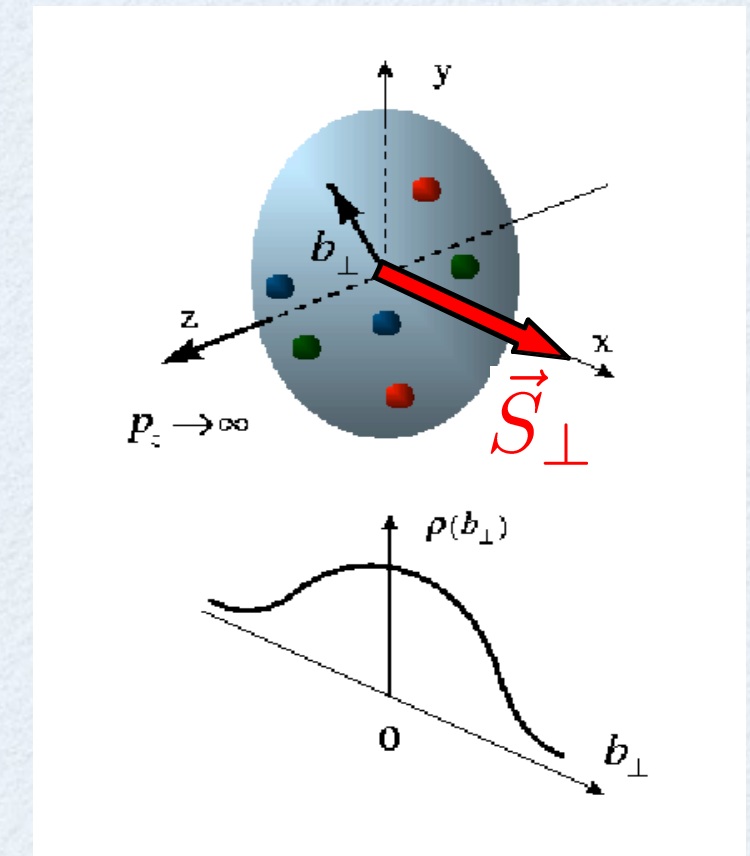
quark transverse charge densities in nucleon (2)

→ **transversely polarized nucleon**

transverse spin $\vec{S}_\perp = \cos \phi_S \hat{e}_x + \sin \phi_S \hat{e}_y$

e.g. along x-axis $\phi_S = 0$

$$\vec{b} = b(\cos \phi_b \hat{e}_x + \sin \phi_b \hat{e}_y)$$



→

$$\begin{aligned} \rho_T^N(\vec{b}) &\equiv \int \frac{d^2 \vec{q}_\perp}{(2\pi)^2} e^{-i \vec{q}_\perp \cdot \vec{b}} \frac{1}{2P^+} \langle P^+, \frac{\vec{q}_\perp}{2}, s_\perp = +\frac{1}{2} | J^+(0) | P^+, -\frac{\vec{q}_\perp}{2}, s_\perp = +\frac{1}{2} \rangle \\ &= \rho_0^N(b) + \sin(\phi_b - \phi_S) \int_0^\infty \frac{dQ}{2\pi} \frac{Q^2}{2M} J_1(bQ) F_2(Q^2) \end{aligned}$$

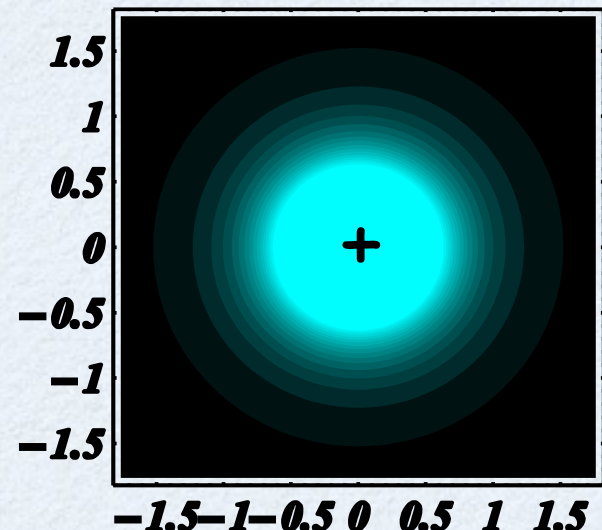


dipole field pattern

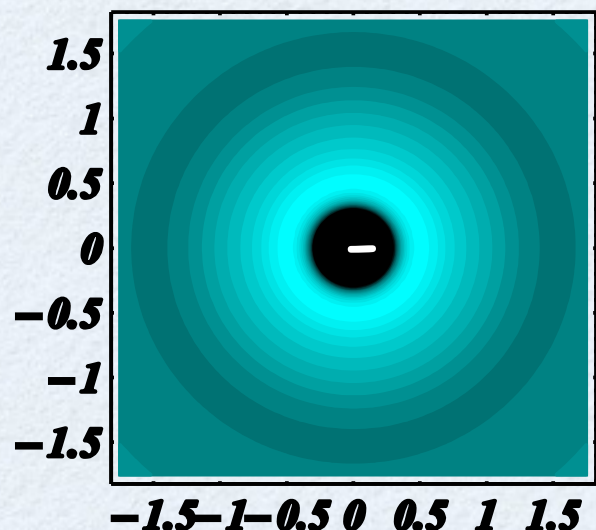
Carlson, vdh (2007)

spatial imaging of hadrons

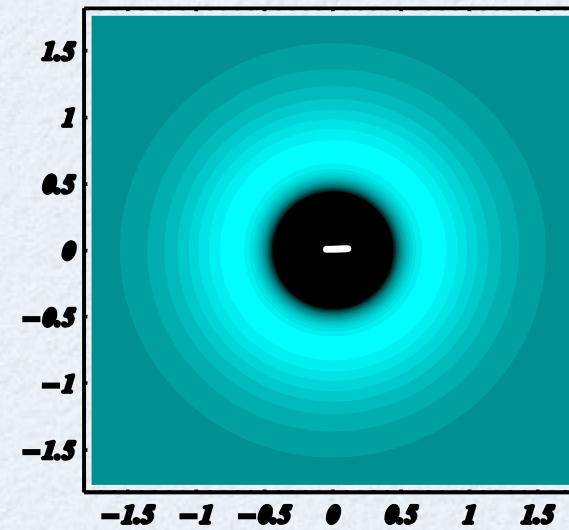
proton



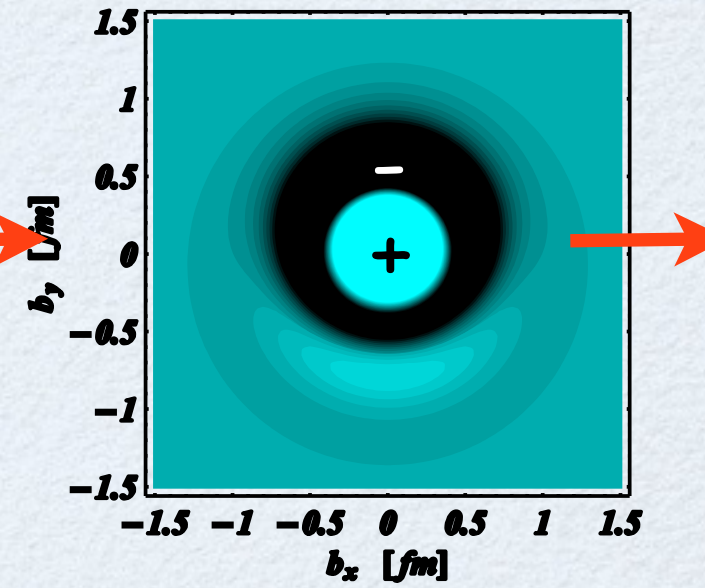
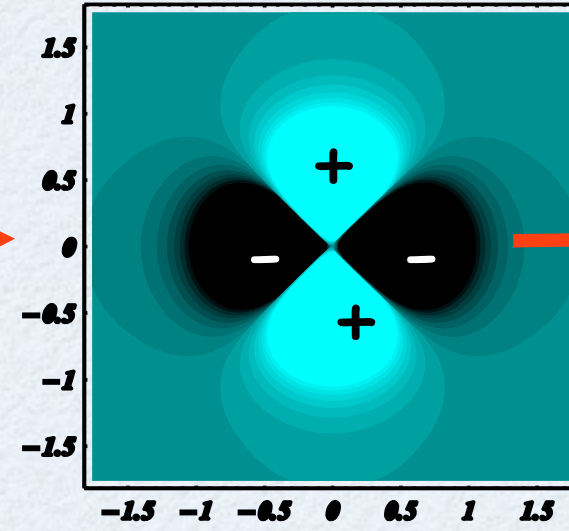
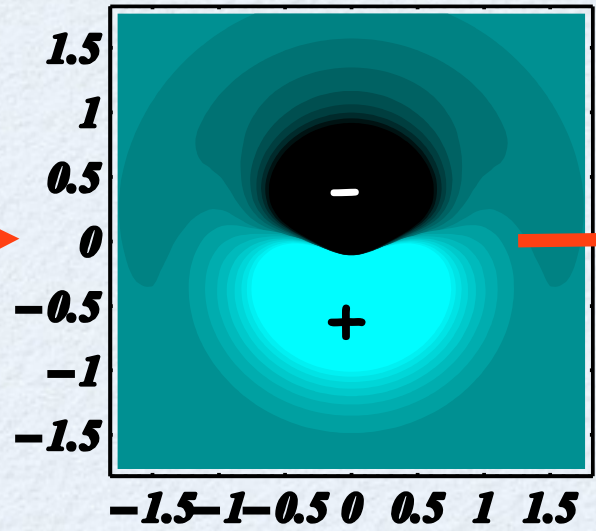
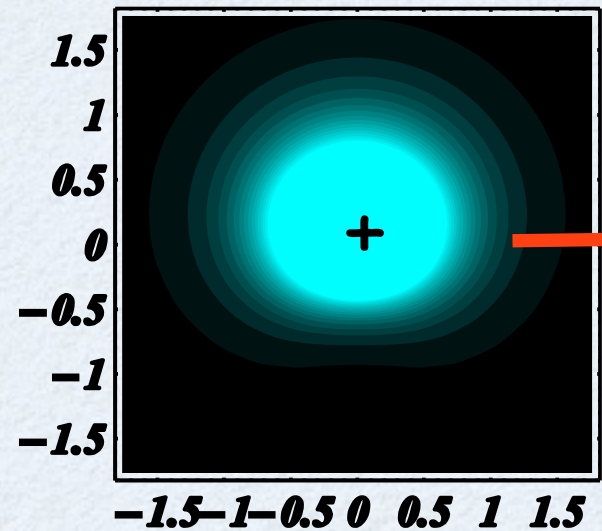
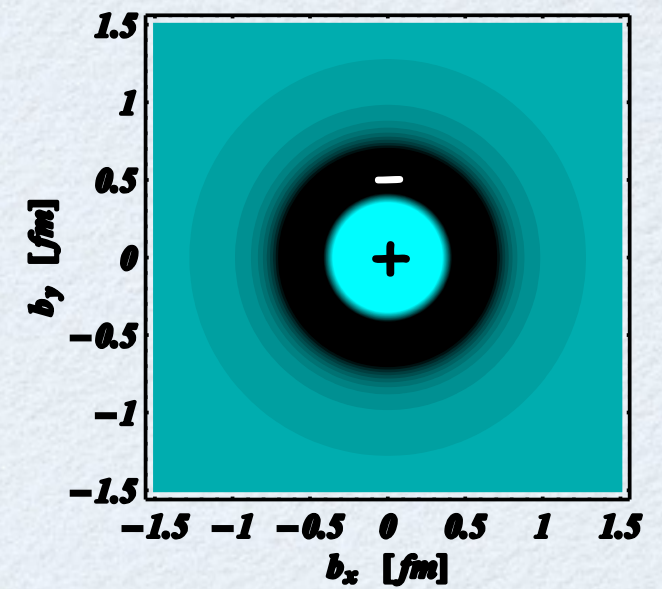
neutron



$p \rightarrow \Delta^+$



$p \rightarrow N^*(1440)$

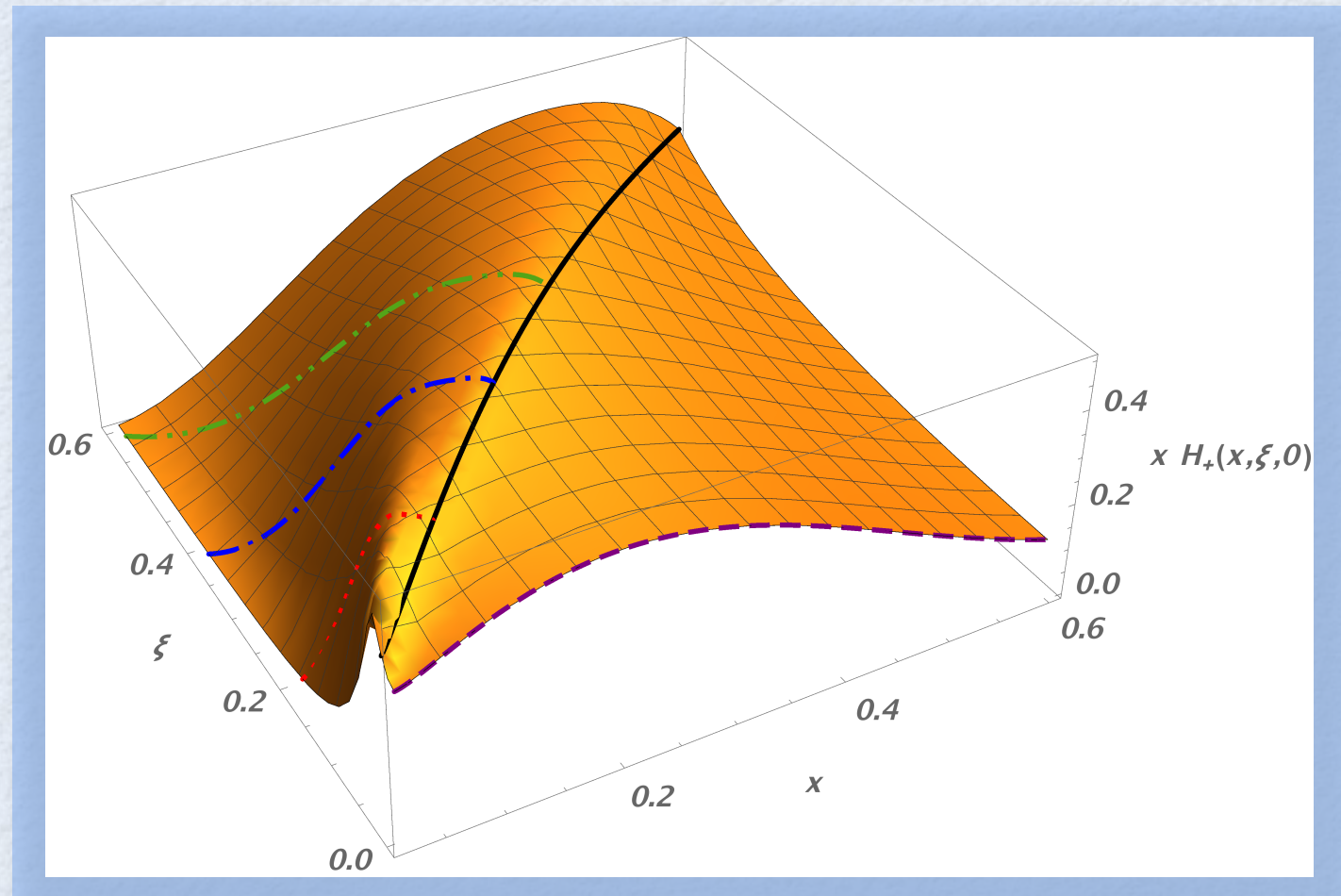


Miller (2007)

Carlson, Vdh (2007)

Tiator, Vdh (2007)

Generalized Parton Distributions



Correlations in transverse position/longitudinal momentum

elastic
scattering



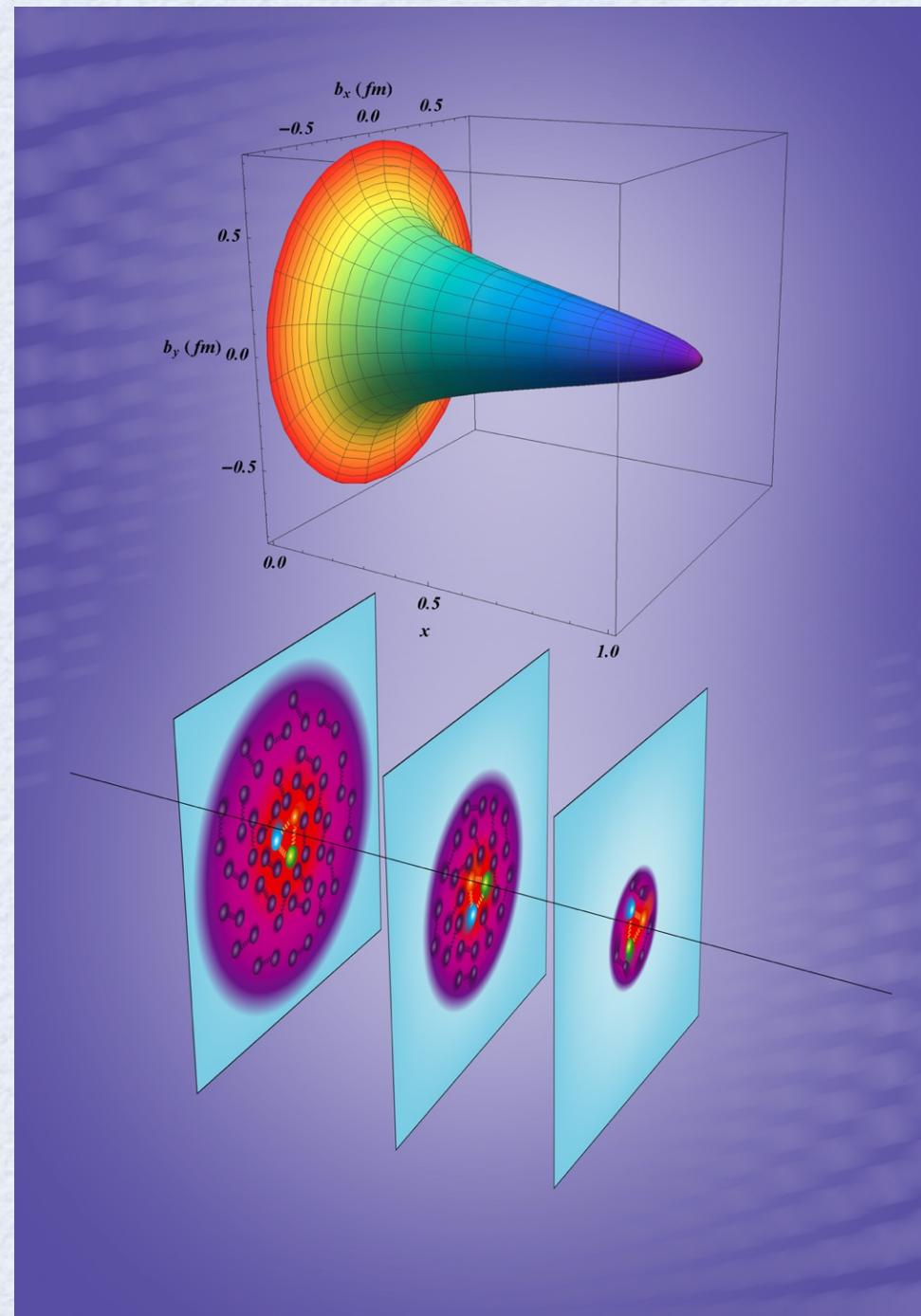
quark
distributions in
transverse
position space

proton
3D imaging

Burkardt (2000, 2003)

Belitsky, Ji, Yuan
(2004)

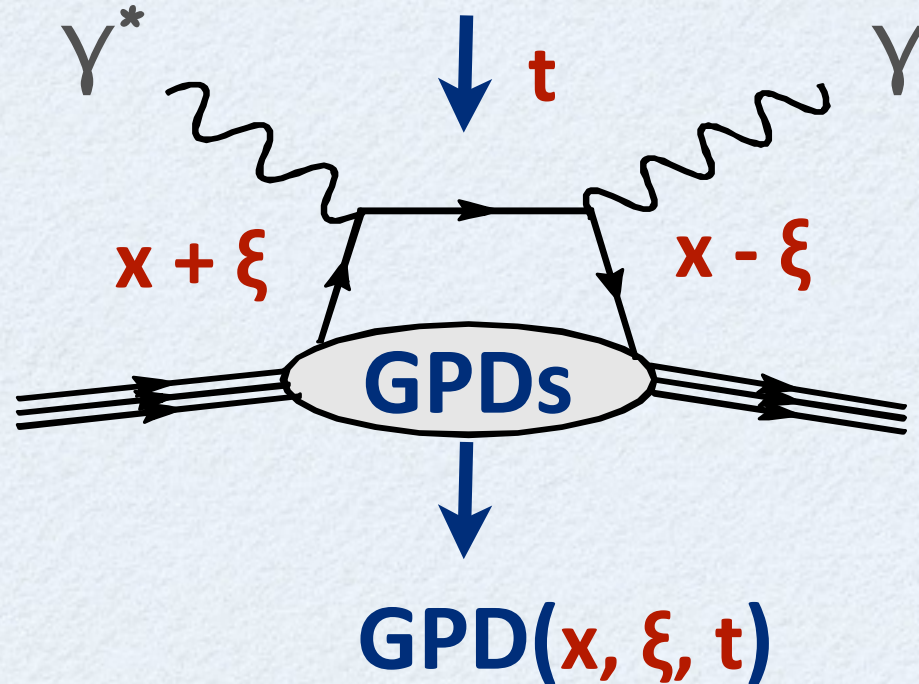
quark
distributions in
longitudinal
momentum



DVCS: tool to access GPDs

world data on proton F_2

$Q^2 \gg 1 \text{ GeV}^2$



→ at large Q^2 : QCD factorization theorem

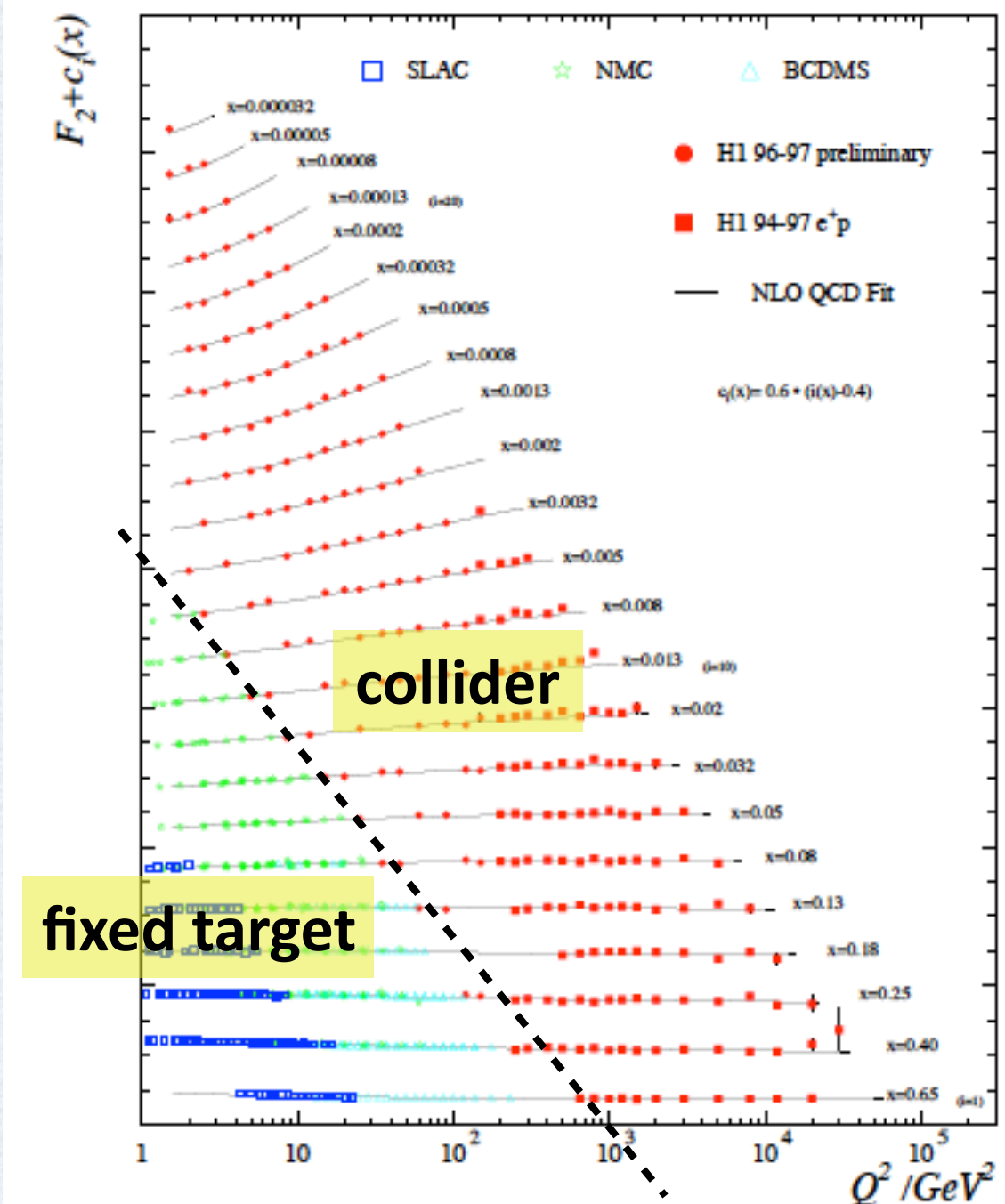
Müller et al (1994)

Ji (1995) Radyushkin (1996)

Collins, Frankfurt, Strikman (1996)

at twist-2: 4 quark helicity conserving GPDs

→ key: Q^2 leverage needed to test QCD scaling



GPDs: known limits

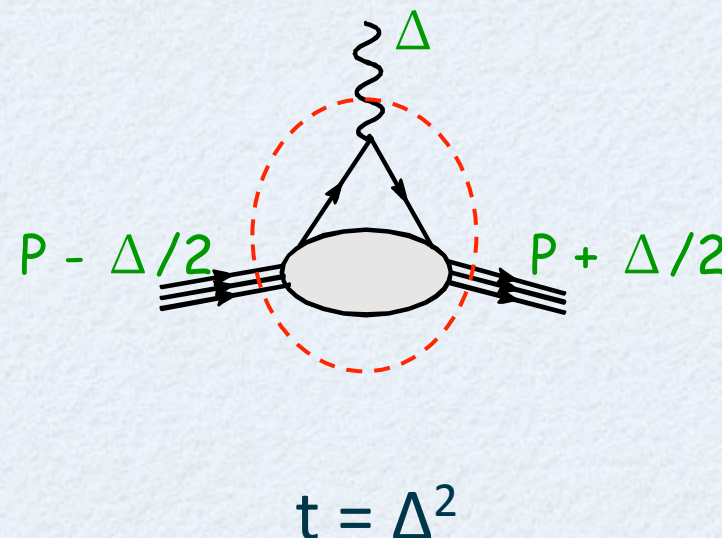
→ in forward kinematics ($\xi=0, t = 0$) : **PDF limit**

$$H^q(x, \xi = 0, t = 0) = q(x)$$

$$\tilde{H}^q(x, \xi = 0, t = 0) = \Delta q(x)$$

E, \tilde{E}^q do not appear in forward kinematics (DIS) → **new information**

→ first moments of GPDs : **elastic form factor limit**



$$\int_{-1}^{+1} dx H^q(x, \xi, t) = F_1^q(t) \rightarrow \text{Dirac FF}$$

$$\int_{-1}^{+1} dx E^q(x, \xi, t) = F_2^q(t) \rightarrow \text{Pauli FF}$$

$$\int_{-1}^{+1} dx \tilde{H}^q(x, \xi, t) = G_A^q(t) \rightarrow \text{axial FF}$$

$$\int_{-1}^{+1} dx \tilde{E}^q(x, \xi, t) = G_P^q(t) \rightarrow \text{pseudoscalar FF}$$

GPDs: moments, total angular momentum



$$\int_{-1}^{+1} dx x H^q(x, \xi, t) = A(t) + \xi^2 C(t)$$

$$\int_{-1}^{+1} dx x E^q(x, \xi, t) = B(t) - \xi^2 C(t)$$

form factors of energy-momentum tensor

Polyakov, Weiss (1999)

Polyakov (2003)



Ji's angular momentum sum rule

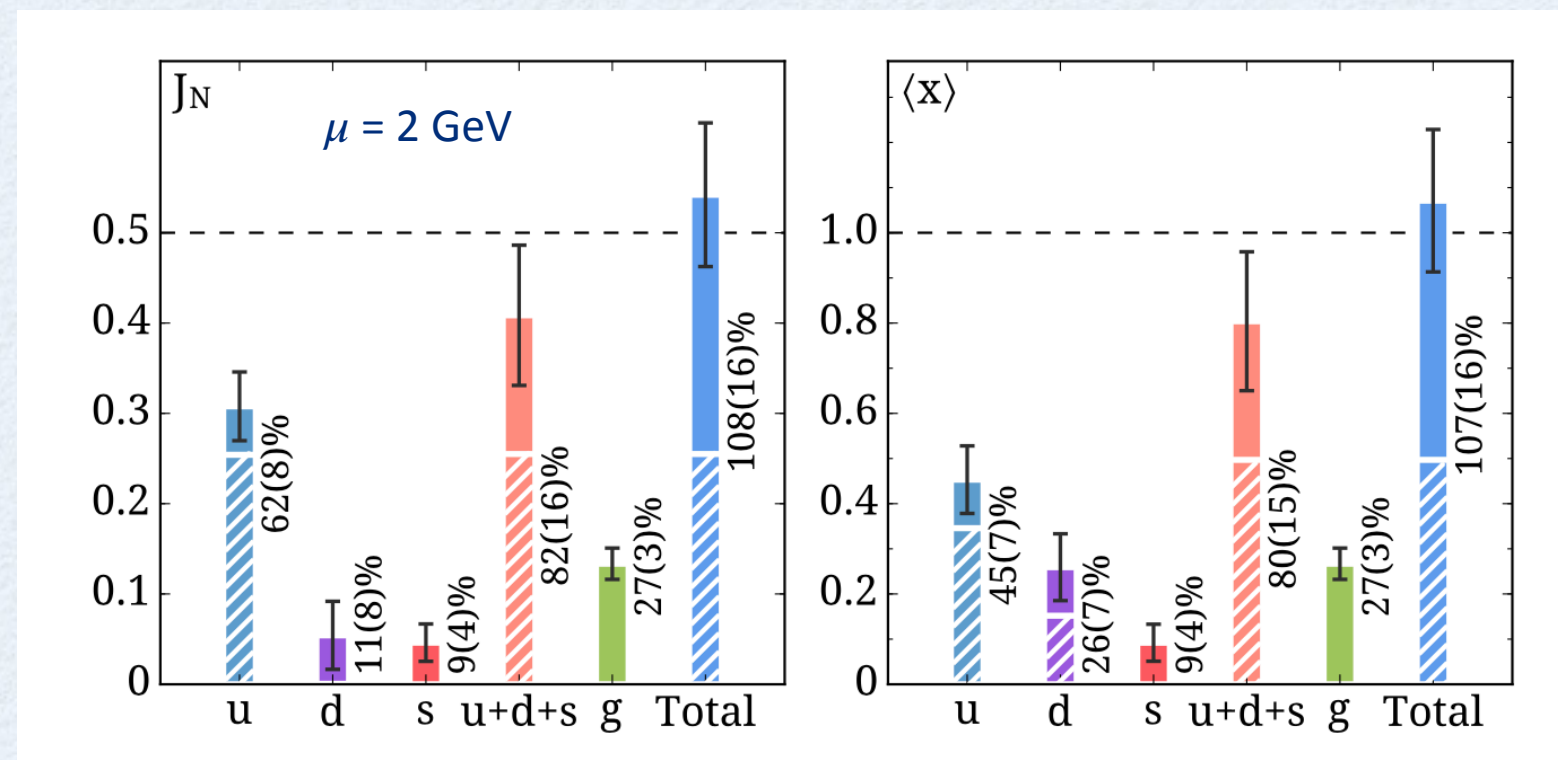
Goeke, Schweitzer et al. (2007)

$$\int_{-1}^{+1} dx x \{ H^q(x, \xi, 0) + E^q(x, \xi, 0) \} = A(0) + B(0) = 2J^q$$



lattice QCD calculations at the physical point

Alexandrou et al. (2017)

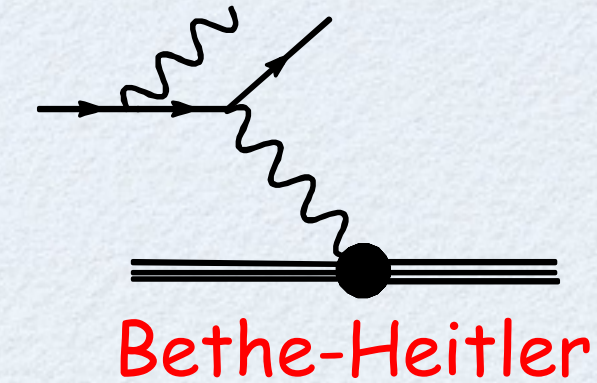
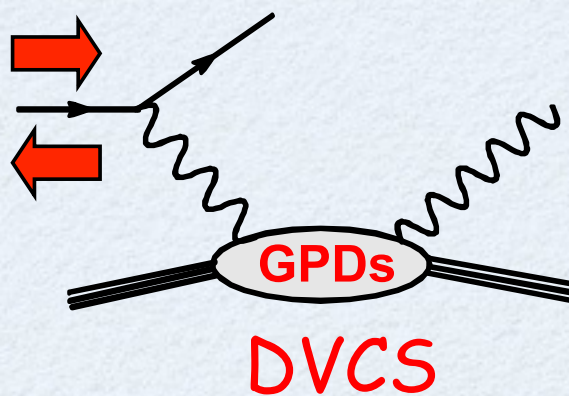


d, s-quarks carry very small total J in proton,
u-quark carries around 60%,
gluons around 30%

Sharing of momentum and total angular momentum between quarks and gluons identical in proton !

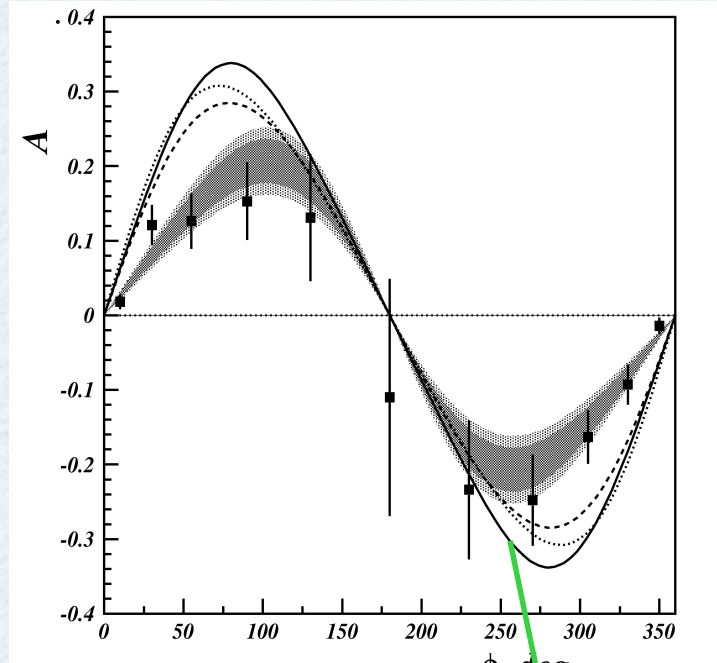
DVCS beam spin asymmetries: first observations around 2000

$$A_{LU} = \frac{(BH) * \text{Im}(DVCS) * \sin \Phi}{(BH^2 + DVCS^2)}$$

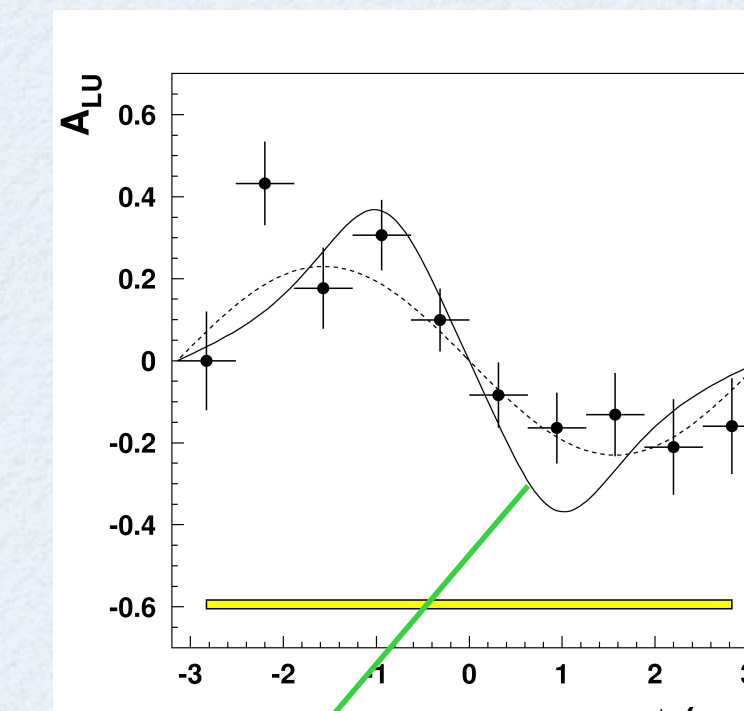


CLAS

$Q^2 = 1.25 \text{ GeV}^2$,
 $x_B = 0.19$,
 $-t = 0.19 \text{ GeV}^2$



PRL 87:182002 (2001)



PRL 87:182001 (2001)

HERMES

$Q^2 = 2.6 \text{ GeV}^2$,
 $x_B = 0.11$,
 $-t = 0.27 \text{ GeV}^2$

twist-2 + twist-3

Vdh, Guichon, Guidal (1999)
Kivel, Polyakov, Vdh (2000)

DVCS accesses Compton Form Factors: 8 CFFs at twist-2



$$\mathcal{H}_{Re}(\xi, t) \equiv \mathcal{P} \int_0^1 dx \left\{ \frac{1}{x - \xi} + \frac{1}{x + \xi} \right\} H_+(x, \xi, t)$$

$$\mathcal{H}_{Im}(\xi, t) \equiv H_+(\xi, \xi, t)$$

$$\tilde{\mathcal{H}}_{Re}(\xi, t) \equiv \mathcal{P} \int_0^1 dx \left\{ \frac{1}{x - \xi} - \frac{1}{x + \xi} \right\} \tilde{H}_+(x, \xi, t)$$

$$\tilde{\mathcal{H}}_{Im}(\xi, t) \equiv \tilde{H}_+(\xi, \xi, t)$$

and analogous formulas for GPDs E, \tilde{E}^q respectively

with singlet GPD combinations
(quark + anti-quark):

$$H_+(x, \xi, t) \equiv H(x, \xi, t) - H(-x, \xi, t)$$

$$\tilde{H}_+(x, \xi, t) \equiv \tilde{H}(x, \xi, t) + \tilde{H}(-x, \xi, t)$$



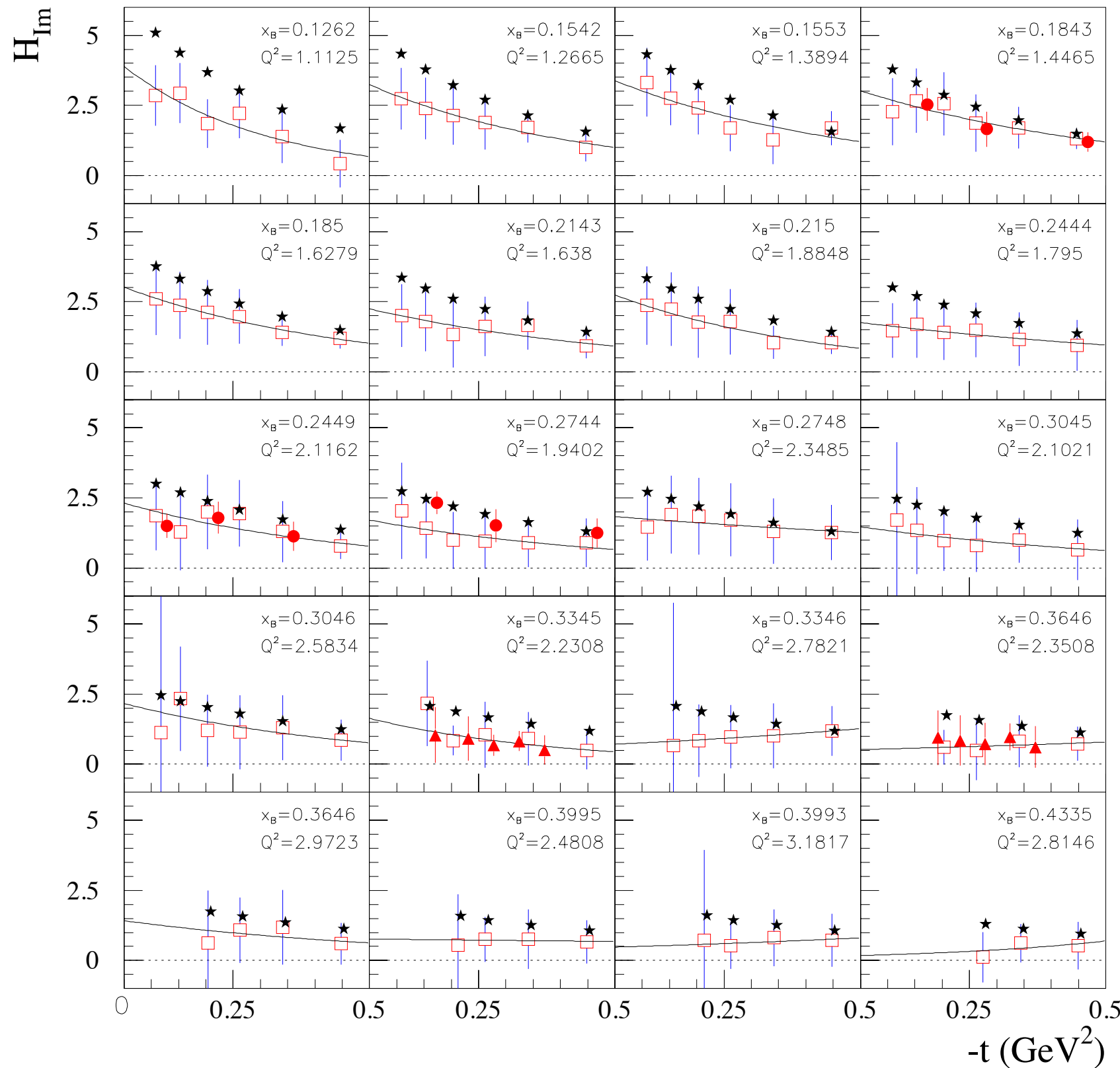
CFF fit extractions from data:

[Guidal \(2008, ...\)](#)

[Guidal, Moutarde \(2009, ...\)](#)

[Kumericki, Mueller, Paszek-Kumericki \(2008, ...\)](#)

global analysis of JLab 6 GeV data



$$\mathcal{H}_{Im}(\xi, t)$$

red solid circles:
CLAS: $\sigma, A_{LU}, A_{UL}, A_{LL}$

red open squares:
CLAS: σ, A_{LU}

red triangles:
Hall A: σ, A_{LU}

black stars
VGG model values

Dupré, Guidal,
vdh (2017)

CFF \mathcal{H}_{Im} :

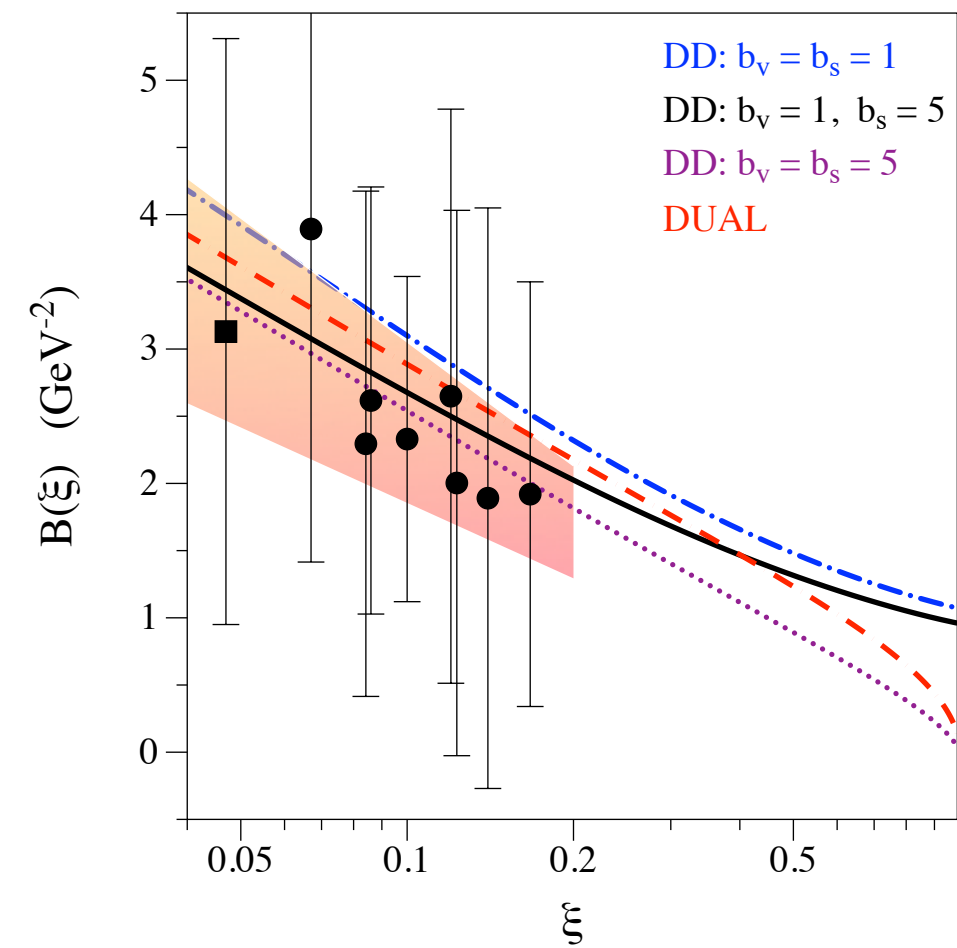
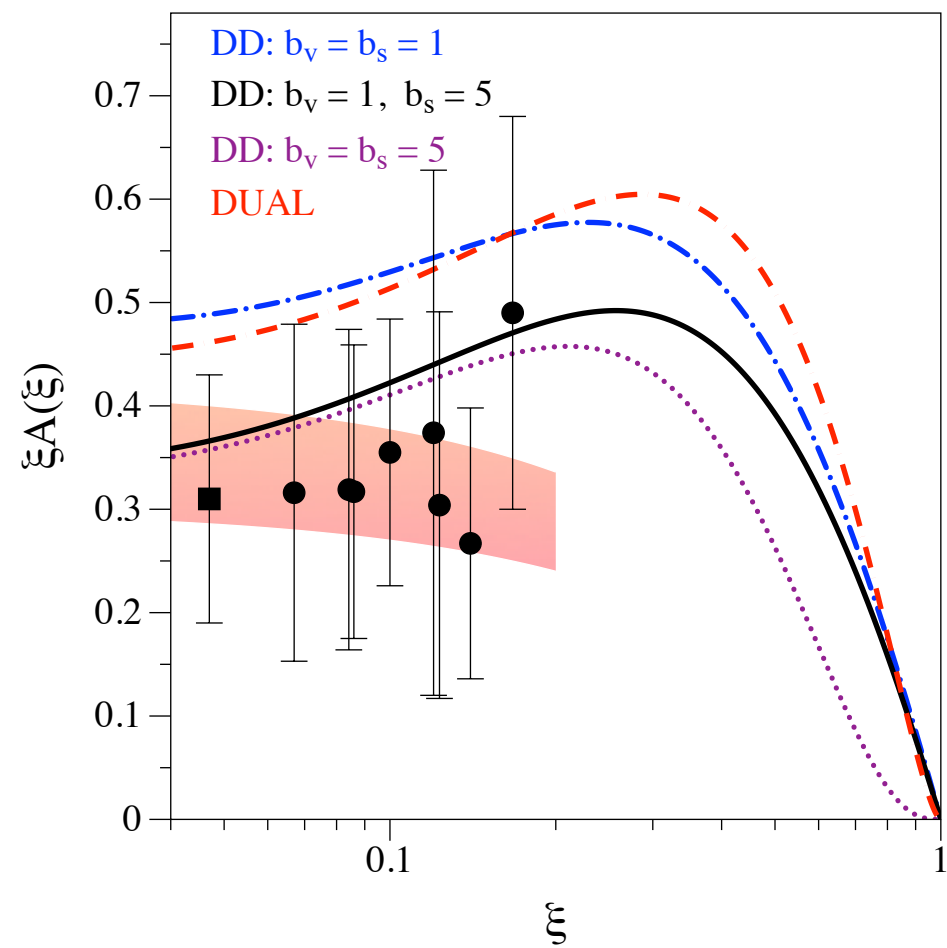
$$\mathcal{H}_{Im}(\xi, t) = A(\xi) e^{B(\xi)t}$$

black circles: CFF fit of JLab data

Dupré, Guidal, Vdh (2017)

black squares: CFF fit of HERMES data

Guidal, Moutarde (2009)



$$A(\xi) = a_A (1 - \xi)/\xi$$

red bands:
1- parameter
fits of data

$$B(\xi) = a_B \ln(1/\xi)$$

3D imaging



$$\rho^q(x, \mathbf{b}_\perp) = \int \frac{d^2 \Delta_\perp}{(2\pi)^2} e^{-i \mathbf{b}_\perp \cdot \Delta_\perp} H_-^q(x, \xi = 0, -\Delta_\perp^2)$$

Burkardt (2000)

number density of quarks (q) with longitudinal momentum x
at a transverse distance \mathbf{b}_\perp in proton



non-singlet (valence quark) GPDs: $H_-^q(x, 0, t) \equiv H^q(x, 0, t) + H^q(-x, 0, t)$



x-dependent radius

$$\langle b_\perp^2 \rangle^q(x) \equiv \frac{\int d^2 \mathbf{b}_\perp \mathbf{b}_\perp^2 \rho^q(x, \mathbf{b}_\perp)}{\int d^2 \mathbf{b}_\perp \rho^q(x, \mathbf{b}_\perp)} = -4 \frac{\partial}{\partial \Delta_\perp^2} \ln H_-^q(x, 0, -\Delta_\perp^2) \Big|_{\Delta_\perp=0}$$

$$H_-^q(x, 0, t) = q_v(x) e^{B_0(x)t} \longrightarrow \langle b_\perp^2 \rangle^q(x) = 4B_0(x)$$



x-independent radius

$$\langle b_\perp^2 \rangle^q = \frac{1}{N_q} \int_0^1 dx q_v(x) \langle b_\perp^2 \rangle^q(x)$$

$N_u=2, N_d=1$

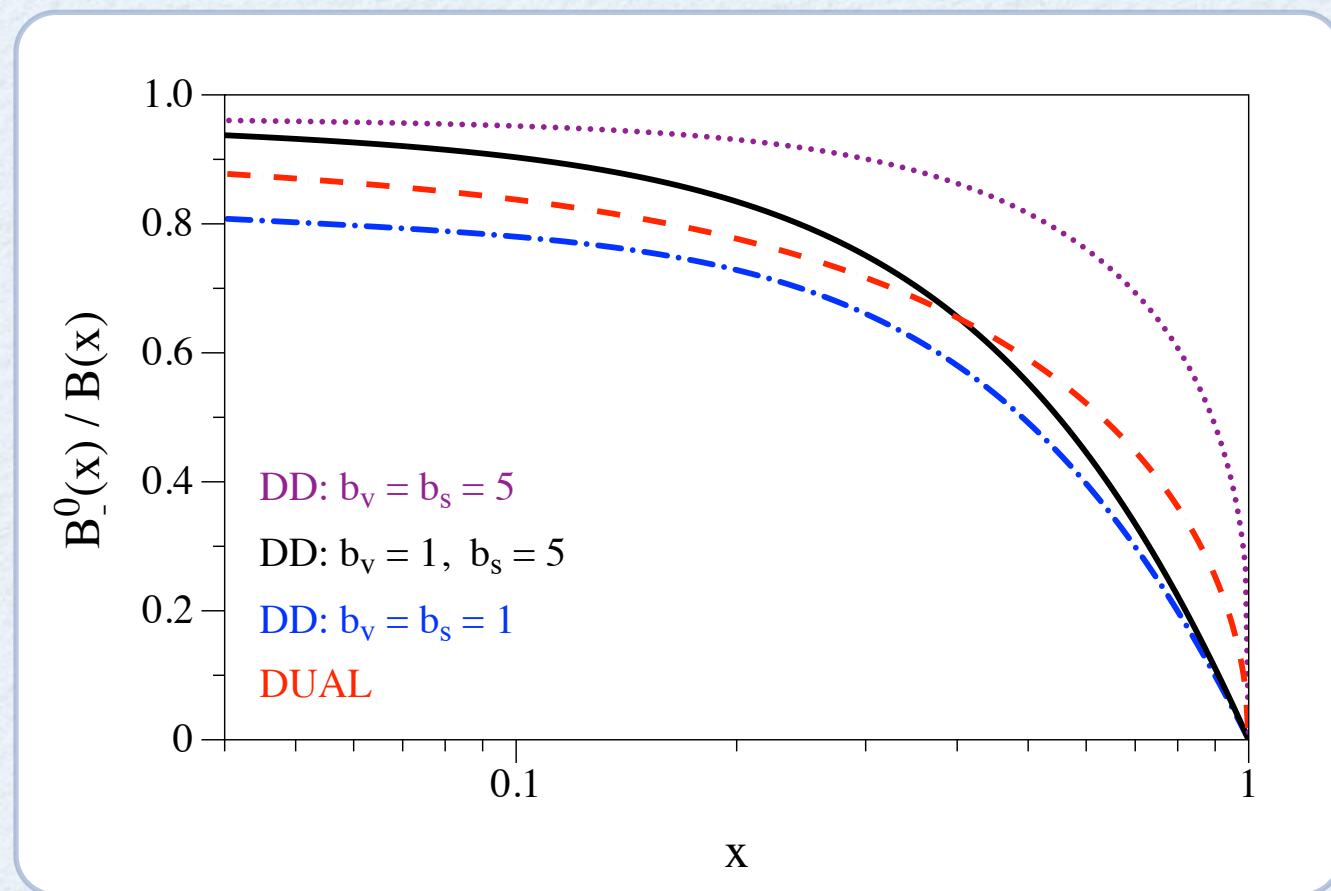
$$\langle b_\perp^2 \rangle = 2e_u \langle b_\perp^2 \rangle^u + e_d \langle b_\perp^2 \rangle^d = 2/3 \langle r_1^2 \rangle = 0.43 \pm 0.01 \text{ fm}^2$$

Bernauer (2014)

x -dependent radius in proton

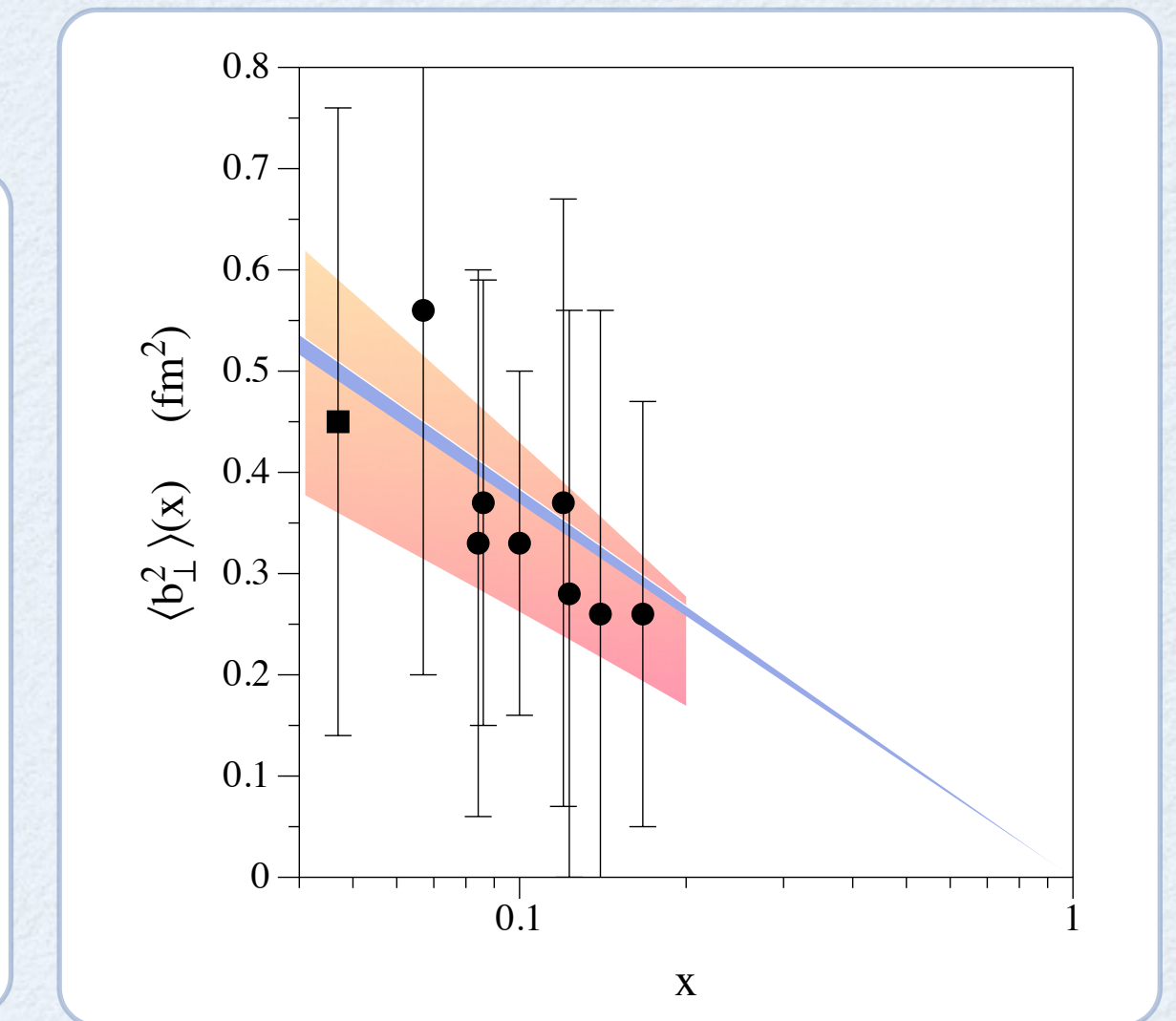
black circles: CFF fit of JLab data

black squares: CFF fit of HERMES data



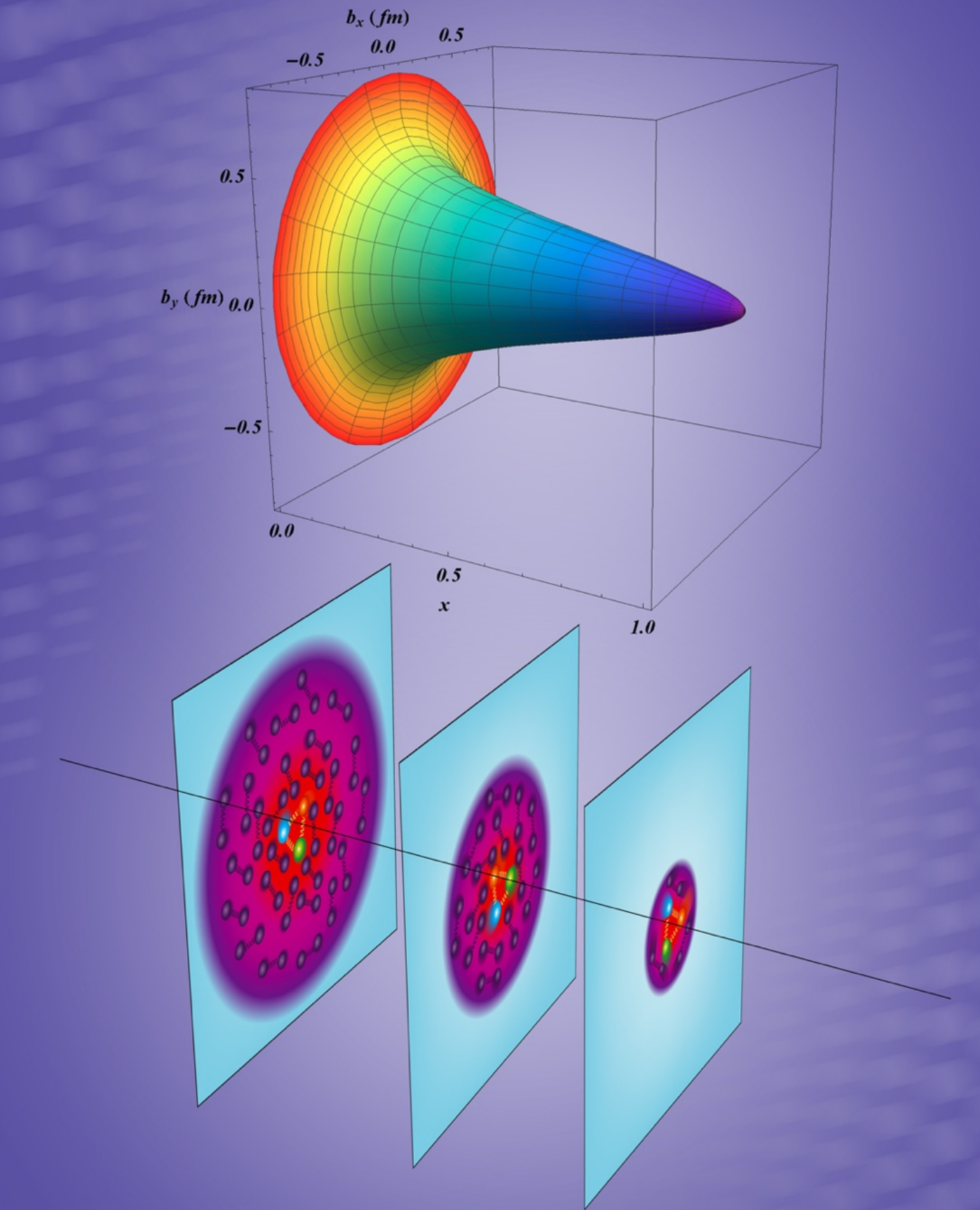
for $x < 0.15$: $B_0 / B > 0.9$

Dupré, Guidal, Niccolai, Vdh (2017)



band: using $B_0(x) = a_{B_0} \ln(1/x)$

a_{B_0} fixed from elastic scattering



3D imaging of proton

Dupré, Guidal, vdh (2017)

CFF \mathcal{H}_{Re} : dispersion relation formalism

Anikin, Teryaev (2007)

Diehl, Ivanov (2007)

Polyakov, Vdh (2008)

Kumericki-Passek, Mueller, Passek (2008)

Goldstein, Liuti (2009)

Guidal, Moutarde, Vdh (2013)

once-subtracted fixed-t dispersion relation

$$\mathcal{H}_{Re}(\xi, t) = -\Delta(t) + \mathcal{P} \int_0^1 dx H_+(x, x, t) \left[\frac{1}{x - \xi} + \frac{1}{x + \xi} \right]$$

ξ -independent subtraction function known from CFF
 $\mathcal{H}_{Im}(x, t)$

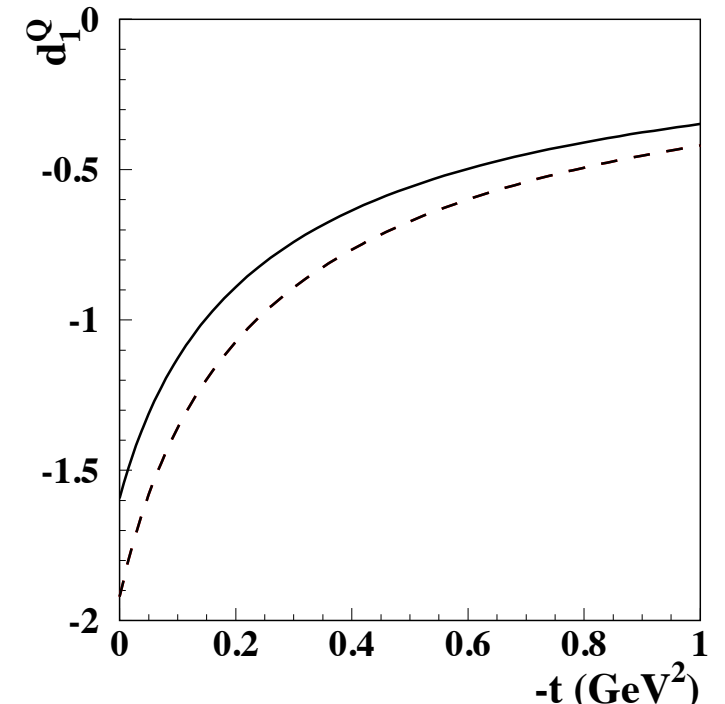
$$\Delta(t) \equiv \frac{2}{N_f} \int_{-1}^1 dz \frac{D(z, t)}{1 - z}$$

D-term

Polyakov, Weiss (1999)

$$D(z, t) = (1 - z^2) \sum_{\substack{n=1 \\ n \text{ odd}}}^{\infty} d_n(t) C_n^{3/2}(z)$$

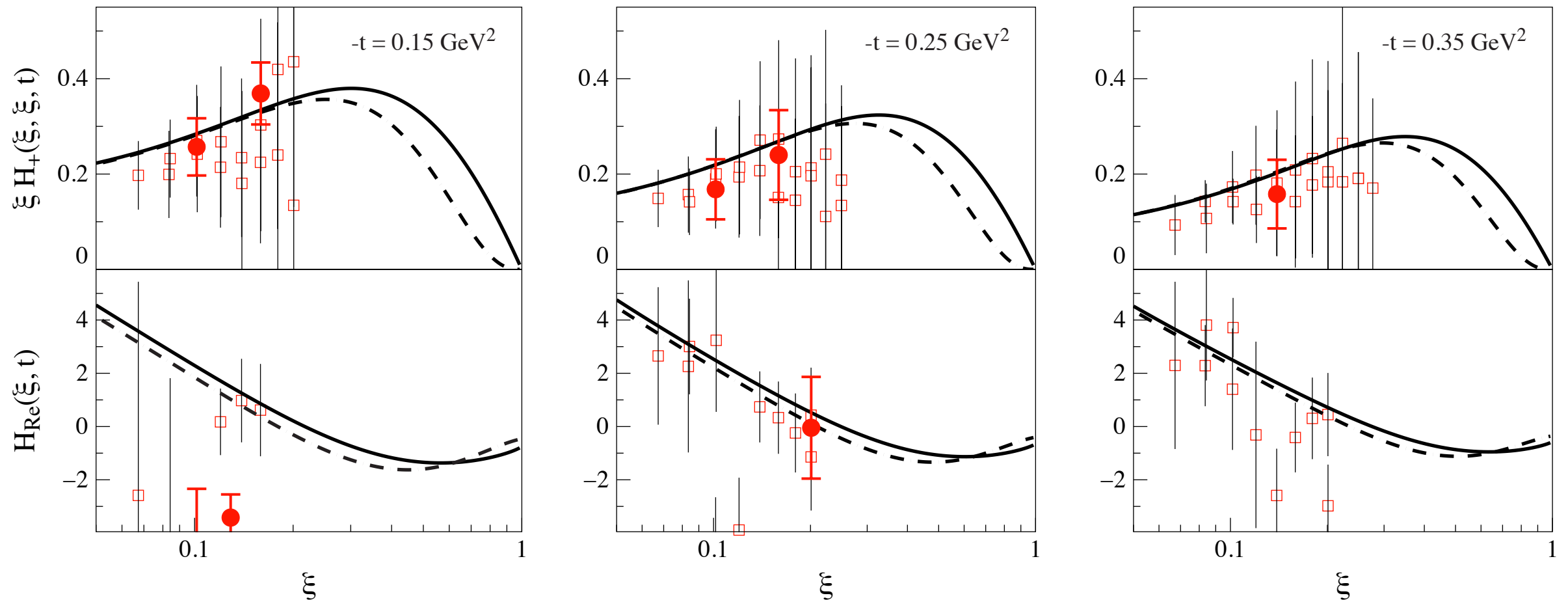
Pasquini, Polyakov, Vdh (2014)



experimental strategy for CFF \mathcal{H}_{Re} : direct extraction vs dispersion formalism

red solid circles: CLAS: $\sigma, A_{LU}, A_{UL}, A_{LL}$

red open squares: CLAS: σ, A_{LU}

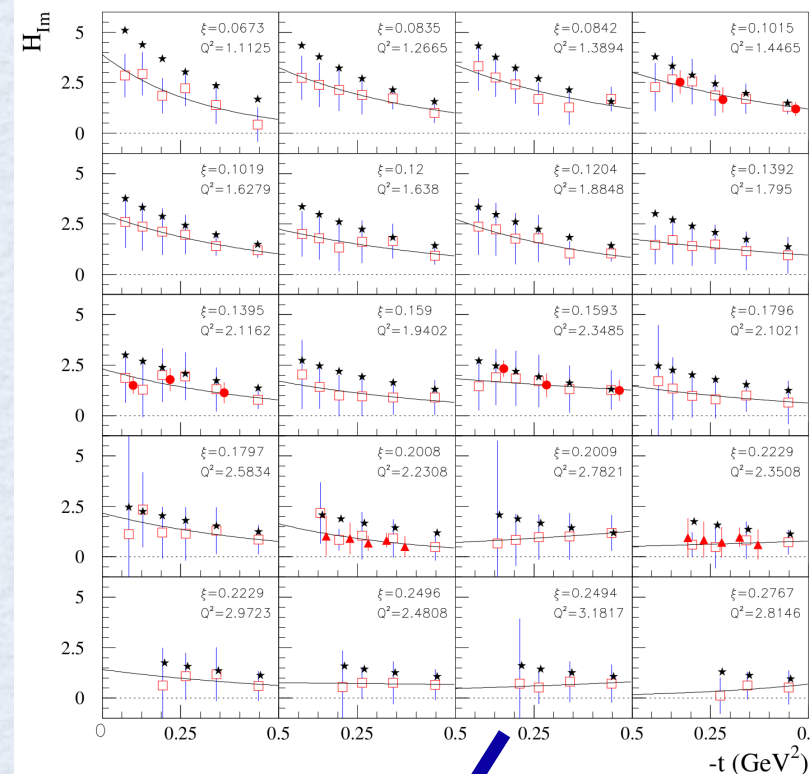


Curves for $\Delta(t) = 0$; $\Delta(t) < 0$ would shift H_{Re} curves up !

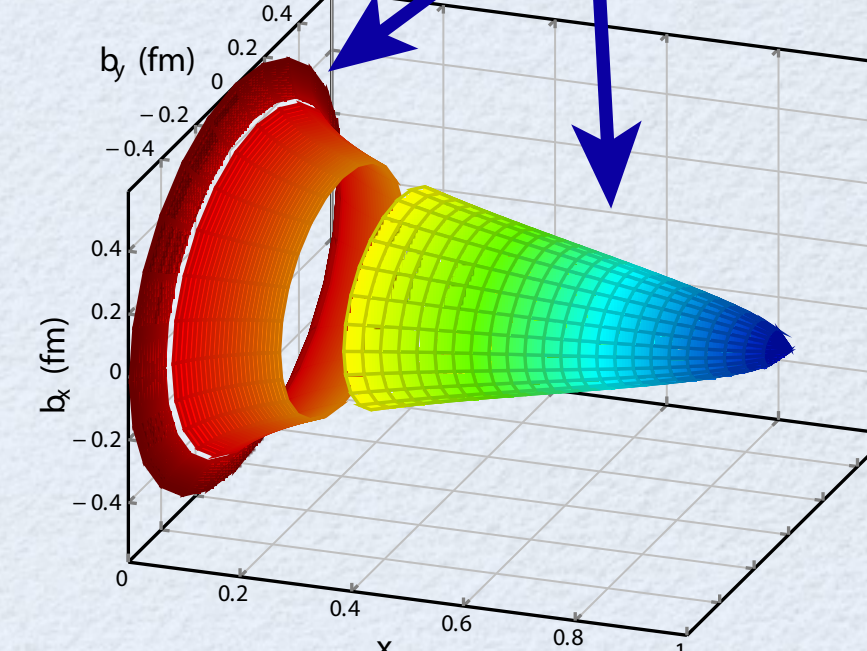
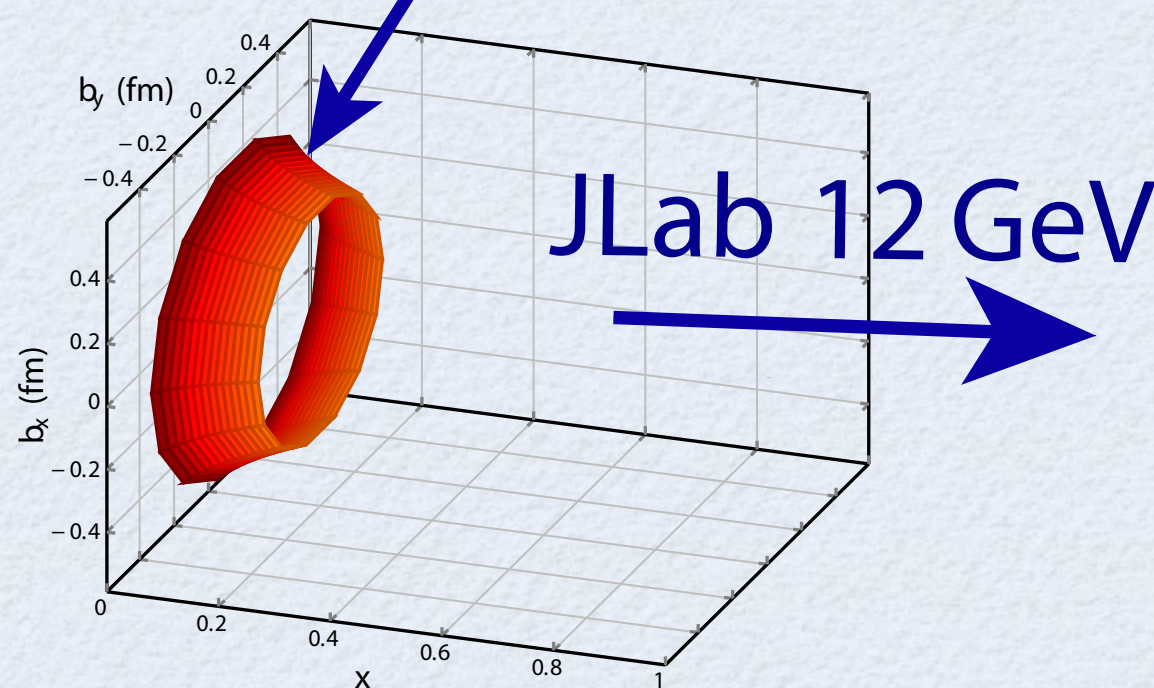
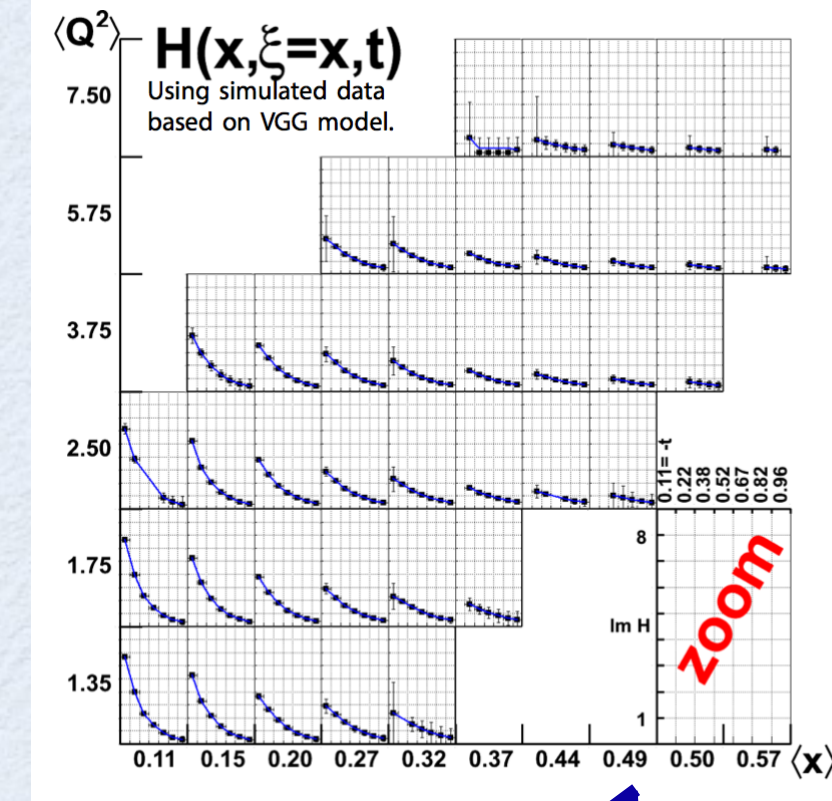
Dupré, Guidal, Niccolai, vdh (2017)

Projections for CFFs at JLab 12 GeV

Düpré-Guidal-Vanderhaeghen-PRD **95** 011501 (R) (2017)



CLAS12 projections E12-06-119 with DVCS A_{UL} and A_{LU}



courtesy of Z.E. Meziani

Outlook

- ➡ elastic / transition FFs have allowed to get a first glimpse at the spatial distributions of quarks in nucleons
- ➡ GPDs allow for a proton imaging in longitudinal momentum and transverse position
- ➡ global analysis of JLab 6 GeV data have shown a proof of principle of such 3D imaging (tools available: fitters, dispersive analyses)
- ➡ systematic 3D imaging is possible now: COMPASS, JLab 12 GeV,...EIC

